THE UNIVERSITY of EDINBURGH

Edinburgh Research Explorer

Contrasting SeaAir CO2 Exchanges in the Western Tropical Atlantic Ocean

Citation for published version:
Monteiro, T, Batista, M, Henley, S, Machado, EDC, Araujo, M & Kerr, R 2022, 'Contrasting SeaAir CO2 Exchanges in the Western Tropical Atlantic Ocean', *Global Biogeochemical Cycles*, vol. 36, no. 8, e2022GB007385. https://doi.org/10.1029/2022GB007385

Digital Object Identifier (DOI):
10.1029/2022GB007385

Link:
Link to publication record in Edinburgh Research Explorer

Document Version:
Peer reviewed version

Published In:
Global Biogeochemical Cycles

General rights
Copyright for the publications made accessible via the Edinburgh Research Explorer is retained by the author(s) and / or other copyright owners and it is a condition of accessing these publications that users recognise and abide by the legal requirements associated with these rights.

Take down policy
The University of Edinburgh has made every reasonable effort to ensure that Edinburgh Research Explorer content complies with UK legislation. If you believe that the public display of this file breaches copyright please contact openaccess@ed.ac.uk providing details, and we will remove access to the work immediately and investigate your claim.

OPEN ACCESS

Download date: 20. Nov. 2022

Contrasting sea-air CO_2 exchanges in the western Tropical Atlantic Ocean

Thiago Monteiro[1,2,3*], Matheus Batista[1,4], Sian Henley[5], Eunice da Costa Machado[1,4], Moacyr Araujo[6,7] and Rodrigo Kerr[1,2,3]

[1]Programa de Pós-Graduação em Oceanologia, Instituto de Oceanografia, Universidade Federal do Rio Grande (FURG), Av. Itália km 8, Rio Grande, 96203-900, RS, Brazil.

[2]Laboratório de Estudos dos Oceanos e Clima, Instituto de Oceanografia, Universidade Federal do Rio Grande (FURG), Av. Itália km 8, Rio Grande, 96203-900, RS, Brazil.

[3]Brazilian Ocean Acidification Network (BrOA), Rio Grande, 96203-900, RS, Brazil

[4]Laboratório de Hidroquímica, Instituto de Oceanografia, Universidade Federal do Rio Grande (FURG), Av. Itália km 8, Rio Grande, 96203-900, RS, Brazil

[5]School of GeoSciences, University of Edinburgh, Edinburgh, EH9 3FE, United Kingdom

[6]Departmento de Oceanografia (DOCEAN), Universidade Federal de Pernambuco (UFPE), Recife, 50740-550, Brazil

[7]Brazilian Research Network on Global Climate Change (Rede CLIMA), São José dos Campos, 12227-010, Brazil

*Corresponding author
Thiago Monteiro
Email: thiagomonteiro@furg.br

Key points

- Sea-air CO_2 release (uptake) shown in the North Brazil Current (North Equatorial Current) domain.
- Strong CO_2 uptake under the Amazon River plume influence, which accounts for 87% of the CO_2 uptake by the western Tropical Atlantic Ocean.
- Increasing trend of sea surface CO_2 partial pressure in the North Brazil Current and the North Equatorial Current waters.

Abstract

The western Tropical Atlantic Ocean is a biogeochemically complex region due to the structure of the surface current system and the large freshwater input from the Amazon River coupled with the dynamics of precipitation. Such features make it difficult to understand the dynamics of the carbon cycle, leading to contrasting estimates in sea-air CO_2 exchanges in this region. Here we demonstrate that these contrasting estimates occur because the western Tropical

This article has been accepted for publication and undergone full peer review but has not been through the copyediting, typesetting, pagination and proofreading process, which may lead to differences between this version and the Version of Record. Please cite this article as doi: 10.1029/2022GB007385.

This article is protected by copyright. All rights reserved.

Accepted Article

Atlantic Ocean can be split into three distinct sub-regions in terms of the sea-air CO_2 exchanges. The sub-region under the North Brazil Current domain acts as a weak annual CO_2 source to the atmosphere, with low interannual variability. The sub-region under the North Equatorial Current influence acts as an annual CO_2 sink, with great temporal variability. The third sub-region under the Amazon River plume influence shows greater interannual variability of CO_2 exchanges, but it always acts as a net oceanic sink for CO_2. Despite this large spatial variability, the entire region acts as a net annual CO_2 sink of -1.6 ± 1.0 mmol m^{-2} day^{-1}. Importantly, the Amazon River plume waters drive 87% of the CO_2 uptake in the western Tropical Atlantic Ocean. In addition, we found a significant increasing trend in sea surface CO_2 partial pressure in the North Brazil Current and North Equatorial Current waters. Such trends are more pronounced than the increase in atmospheric CO_2 partial pressure, revealing the sensitivity of carbon dynamics in these sub-regions to global climate change.

Keywords: CO_2 fluxes; Carbon cycle; Amazon Plume; Northern Brazil Current; North Equatorial Current.

Accepted Article

This article is protected by copyright. All rights reserved.

1 Introduction

The global ocean plays an essential role in regulating atmospheric carbon dioxide (CO_2) levels because it takes up about ~25% of atmospheric CO_2 (Friedlingstein et al., 2020). However, the Tropical Atlantic Ocean is the second largest source of CO_2 from the ocean to the atmosphere, mainly due to equatorial upwelling and warm waters (Landschützer et al., 2014, Takahashi et al., 2009). The ocean dynamics of the surface current system (e.g., Johns et al., 1998; Salisbury, et al., 2011; Johns et al., 2021) and the large freshwater input from the Amazon River (Liang et al., 2020), coupled with precipitation dynamics (Ibánhez et al., 2015; Utida et al., 2019), also add a biogeochemical complexity to the western Tropical Atlantic Ocean (da Cunha & Buitenhuis, 2013). Such complexity is reflected in the pronounced spatial and temporal variability of the marine carbonate system and particularly in the sea-air CO_2 exchanges (Körtzinger, 2003; Cooley et al., 2007; Lefèvre et al., 2010; Valerio et al., 2021; Louchard et al., 2021; Mu et al., 2021). As a result, some sea-air CO_2 flux estimates indicate that the western Tropical Atlantic Ocean acted as a net CO_2 source region (e.g., Cooley et al., 2007; Valerio et al., 2020; Louchard et al., 2021). Conversely, other studies revealed a net CO_2 sink behaviour, mainly due to the high primary productivity driven by optimal nutrient availability supplied by the Amazon River waters (e.g., Körtzinger, 2003; Lefèvre et al., 2010; Ibánhez et al., 2015; Mu et al., 2021). Even when these estimates indicate a sea-air CO_2 flux in the same direction, the magnitude of these fluxes can vary widely among estimates. For example, estimates of sea-air CO_2 exchanges based on satellite data show an average annual CO_2 release of 4.6 mmol m^{-2} day^{-1} (Valerio et al., 2020), while complex biogeochemical models indicate a CO_2 source an order of magnitude lower (0.5 mmol m^{-2} day^{-1}; Louchard et al., 2021) in a vast area of the western Tropical Atlantic. Although most studies indicate that the area under the influence of the Amazon River plume is an important atmospheric CO_2 sink, the magnitude of ocean CO_2 uptake also varies greatly among them (e.g., Mu et al., 2021; Louchard et al., 2021).

This article is protected by copyright. All rights reserved.

The great variability in these fluxes is likely associated with sampling that occurs over a limited period and/or with limited geographic scope that does not capture the full extent of variability across the region. This is particularly true because the spreading area of the Amazon River plume, as well as the period of maximum freshwater discharge, vary seasonally and inter-annually (Liang et al., 2020). Furthermore, the surface current system (e.g., Johns et al., 1998; Salisbury et al., 2011; Johns et al., 2021) and the ocean-atmosphere-land coupling (Utida et al., 2019; Johns et al., 2021; Louchard et al., 2021) make it difficult to build an overall picture of sea-air CO_2 exchanges in this region from spatial and temporal snapshots.

1.1 Oceanographic features of the western Tropical Atlantic Ocean

Surface dynamics in the western Tropical Atlantic Ocean are characterised by a complex system of ocean currents (Fig. 1). The North Equatorial Current (NEC) flows westwards in the northern hemisphere, carrying relatively cold waters from the North Atlantic to the western Tropical Atlantic Ocean (Fig. 1c) (Johns et al., 2021). On the other hand, the North Brazil Current (NBC) flows northwest along the Brazilian coast (Stramma et al., 1995; Rodrigues et al., 2007; Silva et al., 2009), carrying warm and more saline waters (Fig. 1b,c) from the equatorial Atlantic to the northern hemisphere (Johns et al., 1998; Salisbury et al., 2011; Johns et al., 2021). NBC waters reach the Amazon River mouth at approximately 5°N, where intense mixing occurs between marine and riverine waters. North of the Amazon River mouth, the NBC retroflects seasonally (Fig. 1a), carrying waters from both the NBC and the Amazon River plume eastwards into the tropical Atlantic, forming the North Equatorial Countercurrent (NECC) (Fonseca et al., 2004; Garzoli et al., 2004). NECC waters reach the easternmost portion of the western Tropical Atlantic in September-October (Araujo et al., 2017; Lefèvre et al., 2020), when their velocity is maximal (Richardson & Reverdin, 1987), while there are no clear signs of the NECC in the early months of the year (Johns et al., 2021). Moreover, NBC retroflection can lead to the formation of anticyclonic rings (Fig. 1a), which transport waters

This article is protected by copyright. All rights reserved.

with NBC properties to the northwest of the Tropical Atlantic Ocean (e.g., Didden & Schott, 1993; Aroucha et al., 2020). Those eddy-advected waters also carried properties derived from the South Atlantic Ocean, which is influenced by sources in the Indian Ocean (Azar et al., 2021; Orselli et al., 2019), highlighting important inter-ocean and inter-hemispheric transports.

In addition to its complex ocean surface current system, the western Tropical Atlantic Ocean is strongly influenced by freshwater input from the Amazon River (Fig. S1a), which discharges around 6.6 x 10^3 km^3 of riverine water to the western Tropical Atlantic annually (Korosov et al., 2015; Salisbury et al., 2011). As it flows into the ocean, the Amazon River develops a plume that can extend over 10^6 km^2 and reach depths of up to 30-35 m, covering a vast portion of the Tropical Atlantic and reaching up to 30°W and 15°N (Coles et al., 2013). The maximum discharge in the inner portion of the Amazon River mouth occurs in March (Liang et al., 2020) and there is a delay of around 3 months before these waters spread into the western Tropical Atlantic Ocean (e.g., Hellweger & Gordon, 2002; Coles et al., 2013; Korosov et al., 2015). Although the riverine waters reduce the light penetration in this region due to their relatively high sediment loads, there is an extensive reef system around 0° and 49°W (Fig. 1a), which almost confines itself to the Amazon River mouth (Moura et al., 2016). The properties of the Amazon River plume waters influence the solubility of CO_2 (Cooley et al., 2007) and enhance primary production, both of which lead to undersaturation of sea surface CO_2 (Körtzinger, 2003; Ibánhez et al., 2015; Louchard et al., 2021). Thus, the Amazon River plume waters act as a globally relevant atmospheric CO_2 sink (Cooley et al., 2007; Lefèvre et al., 2010; Ibánhez et al., 2015).

This article is protected by copyright. All rights reserved.

Accepted Article

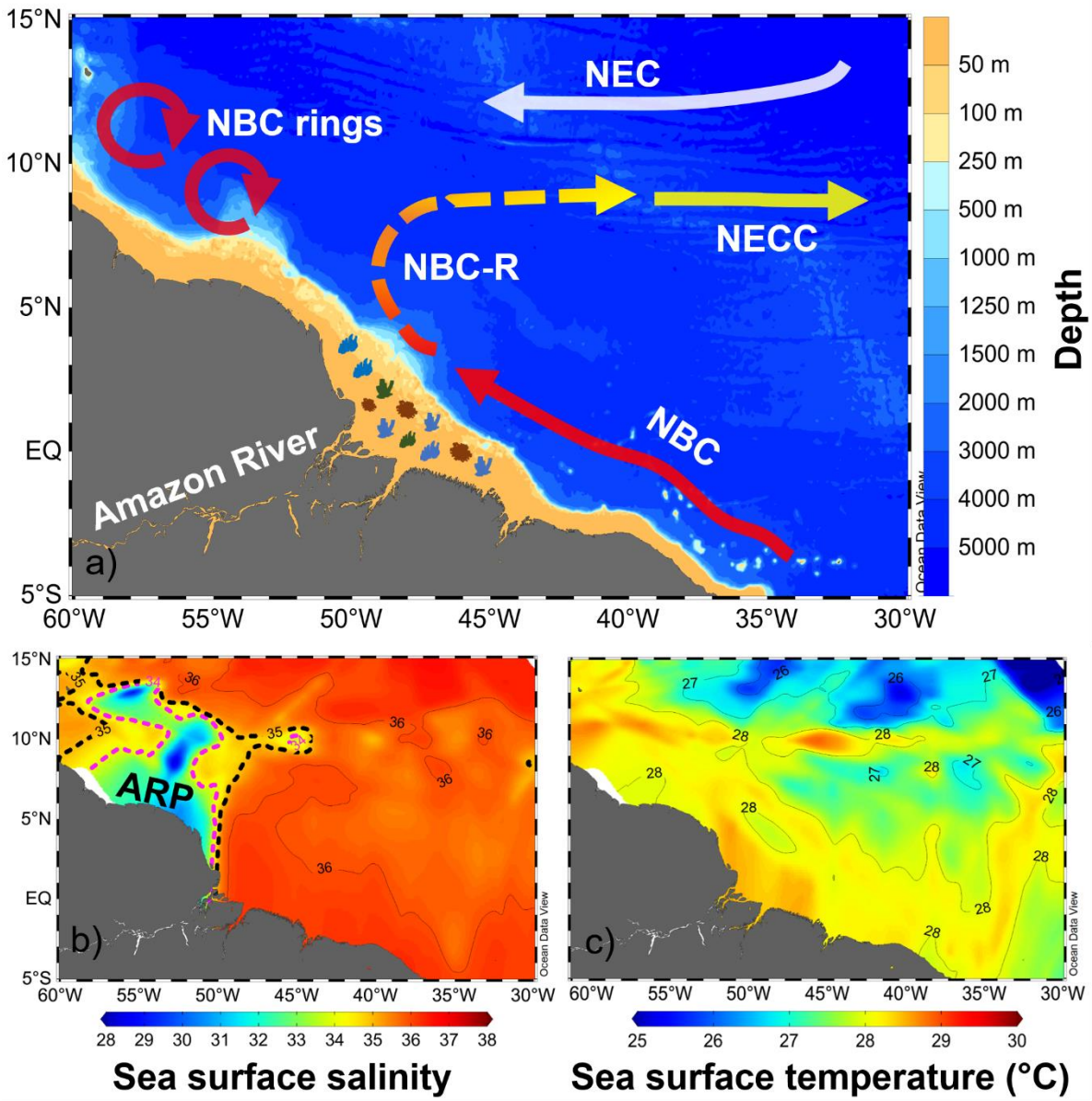

Figure 1: (a) Western Tropical Atlantic Ocean and the main surface currents that characterise the ocean dynamics in this region (see Johns et al., [2021] and references therein): North Equatorial Current (NEC), North Brazil Current (NBC) and the North Equatorial Countercurrent (NECC), which originates from the retroflection of the NBC (NBC-R), as well as the NBC rings. The symbols over the mouth of the Amazon River (a) represent the extensive reef system in this region. (b) Annual climatology of sea surface salinity for the period 1993-2019, with isohalines equal to 35 (dashed black line) and 34 (dashed pink line), representing the Amazon River plume (ARP). (c) Annual climatology of sea surface temperature for the same period in the region.

The intense precipitation (Fig. S1b) driven by the position of the Intertropical Convergence Zone (ITCZ) also influences the ocean dynamics in the western Tropical Atlantic Ocean. The ITCZ varies seasonally, reaching its most northerly position (near 10°N) from June to August and its most southerly (near 4°S) from March to May (Fonseca et al., 2004; Utida et al., 2019), contributing to the seasonal regulation of sea surface salinity. In addition, this region is

This article is protected by copyright. All rights reserved.

influenced by the El Niño–Southern Oscillation (ENSO), which acts to intensify the drought and flooding periods (Marengo & Espinoza, 2016), and by the anomalous warming in the Atlantic Ocean (Tyaquiçã et al., 2017). These events can occur simultaneously, with a range of responses in the physical and chemical properties of the sea surface (Kucharski et al., 2016), adding more complexity to biogeochemical cycles in the western Tropical Atlantic Ocean. Here, we use a broader set of *in situ* data, with improved spatial and temporal coverage compared to any previous study to investigate why there are contrasting results among the estimates of sea-air CO_2 exchanges. Hence, we have gained a more comprehensive understanding of the CO_2 system and its spatial and temporal variability to explain these contrasting estimates of sea-air CO_2 exchanges in the western Tropical Atlantic Ocean.

2 Material and Methods

2.1 Dataset and carbonate system properties

We compiled a time series of the hydrographic and carbonate system parameters from the Surface Ocean CO_2 Atlas version 2020 (SOCAT; Bakker et al., [2016]) in the western Tropical Atlantic Ocean spanning 27 years from 1993 to 2019 (Fig. S2). The variables used included the sea surface (down to a depth of 5 m) temperature (SST), salinity (SSS) and CO_2 partial pressure (pCO_2). The SOCAT represents a synthesis of quality-controlled sea surface CO_2 fugacity data for the global surface oceans and coastal seas with regular updates. Here we used CO_2 fugacity data from SOCAT with uncertainties < 2 µatm (71% of total) and < 5 µatm (29% of total). The CO_2 fugacity data extracted from the SOCAT were measured directly using air-water equilibrators and infrared analysers for CO_2 quantification (Bakker et al., 2016). We converted the CO_2 fugacity data from the SOCAT to pCO_2 using the equations of Weiss (1974). Since SOCAT only provides SST, SSS and pCO_2 data, we determined the sea surface total alkalinity (TA) based on the locally interpolated alkalinity regression (LIAR) approach of Carter et al. (2018), using SST and SSS as input variables. LIAR is a set of linear regressions

This article is protected by copyright. All rights reserved.

capable of estimating TA from different sets of input parameters, considering the depth and coordinates of the measurements. The global uncertainty in the TA estimates using SST and SSS as input variables is expected to be 4.4 µmol kg^{-1} (Carter et al., 2018). The results of LIAR approximations were compared with *in situ* TA data available from GLODAP 2020 (Olsen et al., 2020) in the study region (accuracy of ± 4.0 µmol kg^{-1}) and the root-mean-squared error (RMSE) was 6.5 µmol kg^{-1} (r^2 = 0.99, n = 453, p < 0.0001).

The surface dissolved inorganic carbon (DIC) was determined using CO2Sys v2.1 (Pierrot & Wallace, 2006) based on inputs of SST, SSS, pCO$_2$ and TA, using the HSO_4^- dissociation constant of Dickson (1990) and the total borate-salinity relationship proposed by Uppström (1974). We verified the K1 and K2 constants of Millero et al. (2006), Millero (2010), Lueker et al. (2000), and Mehrbach et al. (1973) refit by Dickson and Millero (1987), as generally recommended for our SSS and SST ranges, and Cai & Wang (1998) for low salinities. The greatest inconsistency for DIC among these constants was 4.64 µmol kg^{-1} between Millero et al. (2006) and Cai and Wang (1998), while the smallest inconsistency was –0.13 µmol kg^{-1} between Lueker et al. (2000) and Mehrbach et al. (1973) refit by Dickson and Millero (1987). These inconsistencies are lower than the error of ± 6.5 µmol kg^{-1} associated with the estimate of TA by the LIAR approximation. Thus, we used the carbonate constants of Millero et al. (2006), which have been widely used in studies in the western Tropical Atlantic Ocean (e.g., Bonou et al., 2016; Araujo et al., 2018).

2.2 Sea-air CO_2 flux

The sea-air CO_2 flux (FCO_2) was calculated by following Eq. (1):

$$FCO_2 = K_t \times K_s \times (p\mathrm{CO}_2^{sw} - p\mathrm{CO}_2^{air}), \quad (1)$$

where K_t is the CO_2 gas transfer velocity, depending on wind speed (Wanninkhof, 2014); K_s is the CO_2 solubility coefficient, as a function of both SST and SSS (Weiss, 1974), pCO$_2^{sw}$ is sea

This article is protected by copyright. All rights reserved.

surface pCO_2 and pCO_2^{air} is atmospheric pCO_2. The pCO_2^{air} was calculated from the monthly averages of the atmospheric molar fraction of CO_2 at Barbados Station located at 13.16°N–59.43°W (Dlugokencky et al., 2021) and atmospheric pressure from SOCAT. The latter was corrected by the water vapour pressure estimated from SST and SSS by the widely used equations of Weiss and Price (1980). We used monthly averages of wind speed (m s^{-1}) at 10 m from the atmospheric reanalysis ERA5 (Fig. S1d) with a spatial resolution of 0.25° (Hersbach et al., 2020). We combined the coordinates and sampling month of the sea surface pCO_2 from SOCAT with the reanalysis ERA5 data to ensure that the wind speed covered the same region and the same period.

The spatial distribution maps for sea-air CO_2 flux, SSS and SST were interpolated using the Ocean Data View function of weighted-average gridding (Schlitzer et al., 2018) to construct the climatologies showed in Figures 1 and 2. We used a length scale value of 20‰ for both the X and Y axes to ensure optimal preservation of data structure and smoothness. The averaging and all other calculations performed in this study were based only on the observed data and not on the interpolated data. We made the map interpolation to provide reader-friendly visualization of the results.

2.3 Drivers of pCO_2 changes

We estimated the drivers of seasonal changes in sea surface pCO_2 (ΔpCO_2^D) between the wet season and the dry season by the approach described in Takahashi et al. (2014), which is based on the seasonal amplitudes of the variables, following Eq. (2):

$$\Delta pCO_2^D = \frac{\partial pCO_2}{\partial DIC}\Delta DIC + \frac{\partial pCO_2}{\partial TA}\Delta TA + \frac{\partial pCO_2}{\partial SST}\ \Delta SST + \frac{\partial pCO_2}{\partial SSS}\Delta SSS\,, \qquad (2)$$

where ΔDIC, ΔTA, ΔSST and ΔSSS are the seasonal amplitudes of the variables (i.e., the difference between averaged values for the wet and dry seasons; Table S2). The partial derivatives are detailed in Supplementary Material (text S3). Here, we used average Revelle

This article is protected by copyright. All rights reserved.

and alkalinity factors of 9.13 and −8.5, respectively. The combined influence of the seasonal drivers is consistent with the calculated ΔpCO_2^D, with an average error of 1 µatm. Here, the seasonal periods were defined as wet (April-September) and dry (October-March) following Bonou et al. (2016), which includes the months when the waters from the Amazon River spread over a larger area throughout the western Tropical Atlantic Ocean in the wet season. There is a delay of up to 3 months from the largest freshwater discharge of the Amazon River to the extreme northwest and east spreading that the freshwater plume can reach (e.g., Hellweger & Gordon, 2002; Coles et al., 2013; Korosov et al., 2015). Therefore, we include both the period of maximum freshwater discharge at the mouth of the Amazon River (Liang et al., 2020) and the months in which its waters reach the easternmost point of the western Tropical Atlantic Ocean (Varona et al., 2019; Lefèvre et al., 2020). To assess the effect of SST on the sea surface pCO_2 time series, we removed its thermal component by normalising pCO_2 to the annual average SST (Eq. 3), following the approach of Takahashi et al. (2002):

$$pCO_{2\,non-thermal} = pCO_{2\,obs} \times \exp\left[0.0423 \times (SST_{avg} - SST_{obs})\right], \qquad (3)$$

where pCO_{2obs} and SST_{obs} are *in situ* sea surface pCO_2 and SST, respectively, and SST_{avg} is the average SST for the entire study period in each sub-region (i.e., NBC-NECC: 27.65 °C, NEC: 26.89 °C, ARP: 28.29 °C).

2.4 Defined sub-regions in the western Tropical Atlantic Ocean

We set the Amazon River plume sub-region (ARP) (i.e., the region under the Amazon River plume domain) to SSS < 35 (Fig. 2) and split the sub-regions under NBC-NECC and NEC domain from a climatology equilibrium isoline of annual average FCO_2 (Fig. S3). Since the FCO_2 equilibrium isoline is expected to oscillate regionally over the time series, we used an average isoline for the entire period, so we can observe the signs of this oscillation in our time series

This article is protected by copyright. All rights reserved.

3 Results

3.1 Regional variability and main drivers of sea-air CO_2 exchanges

We identified three distinct sub-regions for annual sea-air CO_2 flux behaviour in the western Tropical Atlantic Ocean from 1993 to 2019, which are maintained both in dry and wet seasons (Fig. 2). The NBC-NECC sub-region acted as a weak annual source of CO_2 to the atmosphere of 1.5 ± 0.7 mmol m^{-2} day^{-1}, while the NEC acted as a weak annual CO_2 sink of –2.2 ± 1.0 mmol m^{-2} day^{-1} throughout the analysis period. The ARP (i.e., SSS < 35) acted as a moderate CO_2 sink with an annual average of –5.0 ± 3.0 mmol m^{-2} day^{-1}, while a strengthened CO_2 uptake of –10 mmol m^{-2} day^{-1} is observed where the influence of the ARP is intensified (Fig. 2c), mainly during the wet season (Fig. 2b). The sub-region under NBC-NECC influence is outlined by an annual sea-air CO_2 equilibrium isoline around 10°N and is constrained by the ARP sub-region at approximately 50°W. However, the area under the NBC-NECC domain extends beyond 50°W in the dry season and there are signs of its influence beyond 10°N in both the wet and dry seasons (Fig. 2a,b). Moreover, we observed signs of CO_2 outgassing northwest of the ARP sub-region in both dry (Fig. 2a) and wet (Fig. 2b) seasons. The annual ocean CO_2 uptake is intensified in the northwest, and it is reduced in the southern portion of the NEC sub-region. Despite presenting sub-regions with contrasting sea-air CO_2 flux behaviour, the western Tropical Atlantic Ocean behaved as an oceanic CO_2 sink overall from 1993 to 2019 in both wet and dry seasons, with an annual average of –1.6 ± 1.0 mmol m^{-2} day^{-1}. 87% of this CO_2 uptake occurs in waters under the influence of the ARP, as shown by the average CO_2 net flux dropping notably to –0.2 ± 1.0 mmol m^{-2} day^{-1} when the strong CO_2 uptake at the ARP was not considered in the average.

This article is protected by copyright. All rights reserved.

Accepted Article

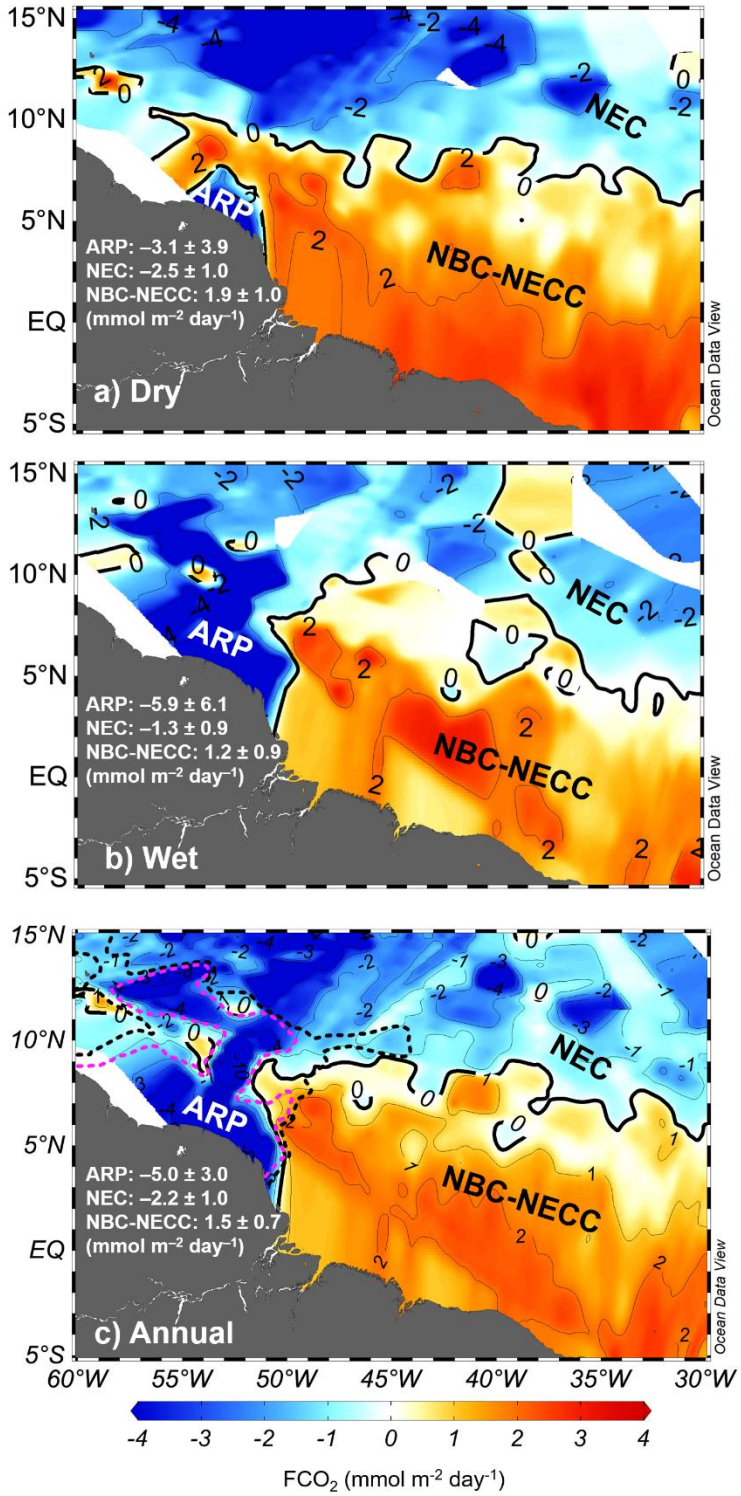

Figure 2: Climatological distribution of the net sea-air CO_2 flux (FCO_2) in the western Tropical Atlantic Ocean from 1993 to 2019 in the **(a)** dry and **(b)** wet seasons, as well as **(c)** annual average. Positive FCO_2 values (yellow to red) represent the outgassing of CO_2 to the atmosphere, whereas negative FCO_2 values (light to dark blue) represent CO_2 uptake by the ocean. There are three distinct sub-regions for FCO_2: the North Brazil Current-North Equatorial Countercurrent (NBC-NECC), acting as a weak source of CO_2 to the atmosphere; the North Equatorial Current (NEC), acting as a weak sink of atmospheric CO_2; and the Amazon River plume (ARP), which is a moderate sink of atmospheric CO_2. The bold black line represents the isoline for FCO_2 equal to zero, where there is an equilibrium in the sea-air CO_2 exchange. The black dashed isoline in **(c)** delimits the region under the influence of the ARP, characterised by salinity < 35 and the pink dashed isoline delimits the region with salinity < 34, where the influence of the Amazon plume is intensified. The numbers indicate the averages and standard deviations of FCO_2 in each sub-region.

This article is protected by copyright. All rights reserved.

Since atmospheric pCO_2 is more stable seasonally than sea surface pCO_2, we consider seasonal variations in sea surface pCO_2 as the main driver of the sea-air CO_2 fluxes. From the dry to the wet season, sea surface pCO_2 increased by 16 µatm in the NEC sub-region, while it decreased by 16 µatm in the ARP sub-region and by only 3 µatm in the NBC-NECC sub-region (Fig. 3). DIC and TA were the main drivers of seasonal variations of sea surface pCO_2 in all sub-regions and SSS was a secondary driver in ARP. Both DIC and TA had the same magnitude but with opposite signs, thus almost counteracting each other's effect on sea surface pCO_2 (Fig. 3a). However, when we normalised DIC and TA to SSS (see text S2 for details), SSS appears as the main driver of sea surface pCO_2 drawdown in the wet season in ARP. Such a pCO_2 drawdown is partially counteracted by an increase in salinity-normalised DIC (nDIC) in the wet season, and the influence of salinity-normalised TA (nTA) and SST is negligible (Fig 3b). A significant difference was observed in NBC-NECC, where nDIC and SSS led to a sea surface pCO_2 drawdown in the wet season, and this was almost counteracted by the increase in SST. The main change by using nDIC and nTA in NEC was the decrease in the magnitude of TA as a sea surface pCO_2 driver, so virtually every increase in sea surface pCO_2 in the wet season was driven by the increase in DIC (Fig 3b).

Accepted Article

This article is protected by copyright. All rights reserved.

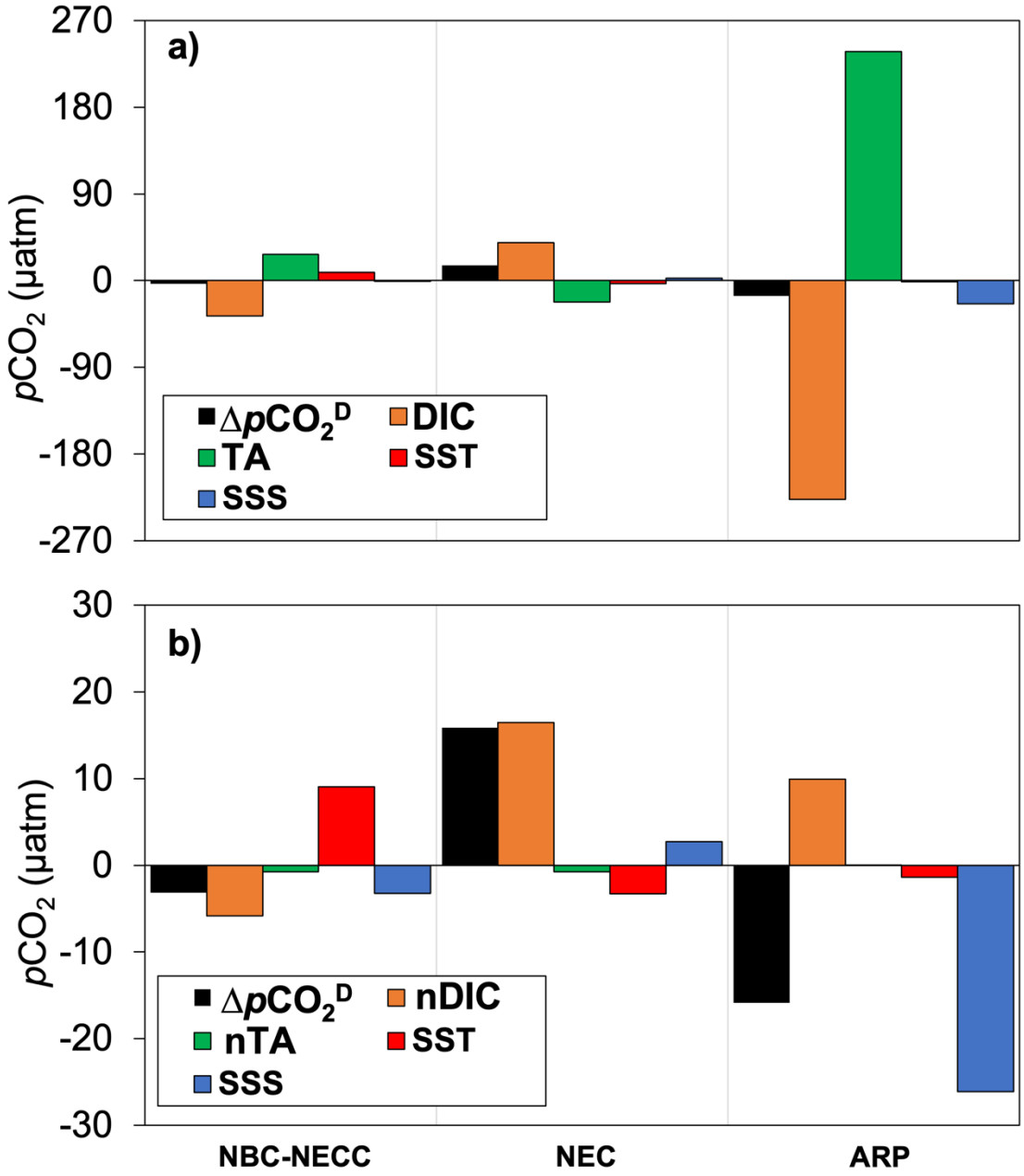

Figure 3: Effects of seasonal variation in total alkalinity (TA), dissolved inorganic carbon (DIC), sea surface temperature (SST) and sea surface salinity (SSS) on the seasonal variation in sea surface pCO_2 (ΔpCO_2^D) for each sub-region of the Western Tropical Atlantic Ocean. In **(a)** the influence of TA and DIC and in **(b)** the influence of TA and DIC normalised to the annual average salinity of each sub-region (nTA and nDIC, respectively), following Friis et al. (2003). The annual average salinities used were 35.87, 34.71 and 31.93 for the North Brazil Current-North Equatorial Countercurrent (NBC-NECC), the North Equatorial Current (NEC), and the Amazon River plume (ARP) sub-regions, respectively. The seasonal variation in each parameter is calculated as the difference between the wet (April – September) mean value and the dry (October – March) mean value. The unit of all drivers is the same as that for pCO_2 (µatm), and their magnitudes represent their influence on pCO_2 changes. Positive values indicate that an increase in the parameter led to an increase in pCO_2; negative values indicate that a decrease in the parameter led to a decrease in pCO_2. The only exception to this is TA because an increase in TA leads to a decrease in pCO_2 and vice versa. The combined influence of the seasonal drivers is consistent with the calculated seasonal variation in pCO_2 (ΔpCO_2^D), with an average error of less than 10%. More details are given in the methods section.

Accepted Article

This article is protected by copyright. All rights reserved.

The dispersion of TA and DIC and the ratio between these parameters can be used to diagnose the processes influencing them (Fig. 4), because each process alters TA and DIC with a certain ratio (Zeebe & Wolf-Gladrow, 2001). Here, the TA:DIC ratio for the whole region was 1.13, very close to the 1.12 ratio expected for the sum of all processes acting together (Fig. 4). This ratio decreases to 0.81 in NEC and to 0.87 in NBC-NECC, revealing that variations in DIC in these sub-regions are likely more important than variations in TA. In fact, when the effect of SSS on TA and DIC is removed, the CO_2 release and uptake processes seem to exert greater influence in waters under the NEC and NBC-NECC domain (Fig. 4b). On the other hand, in the ARP sub-region the TA:DIC ratio was 1.14, likely revealing that all processes controlling TA and DIC act simultaneously. After removing the SSS effect in the ARP sub-region, dissolution and calcification processes exerted greater influence over a wide range of salinity, while photosynthesis (Fig. S8) and CO_2 release/uptake processes can also work to control the changes in nDIC and nTA in waters with salinities < 30 (Fig. 4c).

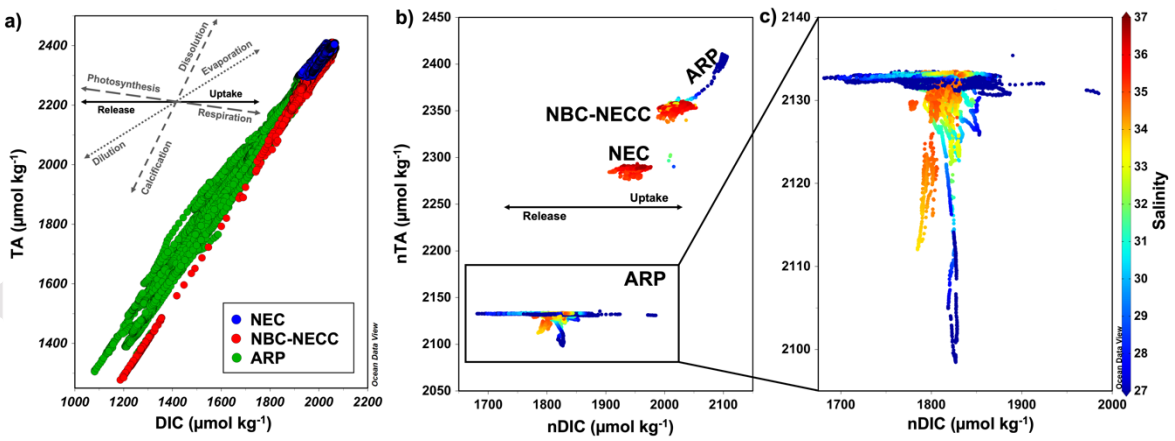

Figure 4: **(a)** Total alkalinity (TA) and dissolved inorganic carbon (DIC) dispersion diagram for the North Brazil Current-North Equatorial Countercurrent (NBC-NECC), North Equatorial Current (NEC), and Amazon River plume (ARP) sub-regions. In **(b)** the diagram is shown considering TA and DIC normalised by the annual average salinity of each sub-region (nTA and nDIC, respectively), following Friis et al. (2003) and in **(c)** the same only for ARP. The annual average salinities used were 35.87, 34.71 and 31.93 for the sub-regions NBC-NECC, NEC and ARP, respectively. The arrows represent the TA:DIC (nTA:nDIC) ratio that characterises the physical-biogeochemical processes that affect these parameters (based on Zeebe & Wolf-Gladrow, 2001) and the colourbar indicates salinity in (b) and (c). Such TA:DIC ratios are as follows: 2:1 for calcification/dissolution, 6:5 for dilution/evaporation, -0.14:1 for photosynthesis/respiration, whereas only DIC is altered in release/uptake processes. Note that the axis scales are different among subplots.

This article is protected by copyright. All rights reserved.

3.2 Temporal variability and trends in sea-air CO_2 exchanges

From 1993 to 2019, the temporal variability of the carbonate system parameters and SSS follow similar oscillation and lower amplitude in both NBC-NECC and NEC sub-regions, while much larger interannual variability occurs in the ARP domain (Fig. 5). On the other hand, SST was the parameter that varied most in NBC-NECC and NEC over the period studied, with amplitude similar to that of ARP (Fig. 5c). SSS, pCO_2, DIC and TA were markedly higher in NBC-NECC and NEC than in ARP. In the NBC-NECC and NEC sub-regions, sea surface pCO_2 increased significantly at a rate of 2.27 and 2.23 µatm year^{-1} from 1993 to 2019, respectively (Fig. 5a). This resulted in a sea surface pCO_2 increase of 59 µatm at NBC-NECC and 58 µatm at NEC over the 27-year study period. Such an increasing trend was also observed in the time series of sea surface pCO_2 anomaly in both sub-regions (Fig. S4) and in both wet and dry seasons (Fig. S5). SST showed a significant increase of 0.06°C year^{-1} in the NEC sub-region, when the anomalous year 2002 (i.e., the warmest year in the time series) is removed (Fig. 5c). DIC also increased at a rate of 1.22 µmol kg^{-1} year^{-1} in NBC-NECC sub-region (Fig. 5e). All hydrographic and carbonate variables showed marked interannual variability in ARP, without any statistically significant trend. The highest interannual amplitude of sea surface pCO_2 in ARP (84 µatm) was found between 2012 and 2017, concurrent with higher amplitudes in SSS (4.67), TA (259 µmol kg^{-1}) and DIC (232 µmol kg^{-1}). Despite the significant steady increase in sea surface pCO_2 in NBC-NECC and NEC, there was no significant trend in sea-air CO_2 exchanges in these sub-regions (Fig. 5f). On the other hand, CO_2 uptake in ARP showed a slight increase of –0.21 mmol m^{-2} day^{-1} over the time series, at the 94% confidence level (Fig. 5f). Over the 27-year study period, these sub-regions maintained their average behaviour as a source (NBC-NECC) or sink (NEC and ARP) of CO_2, with variations only in the magnitude of these fluxes.

This article is protected by copyright. All rights reserved.

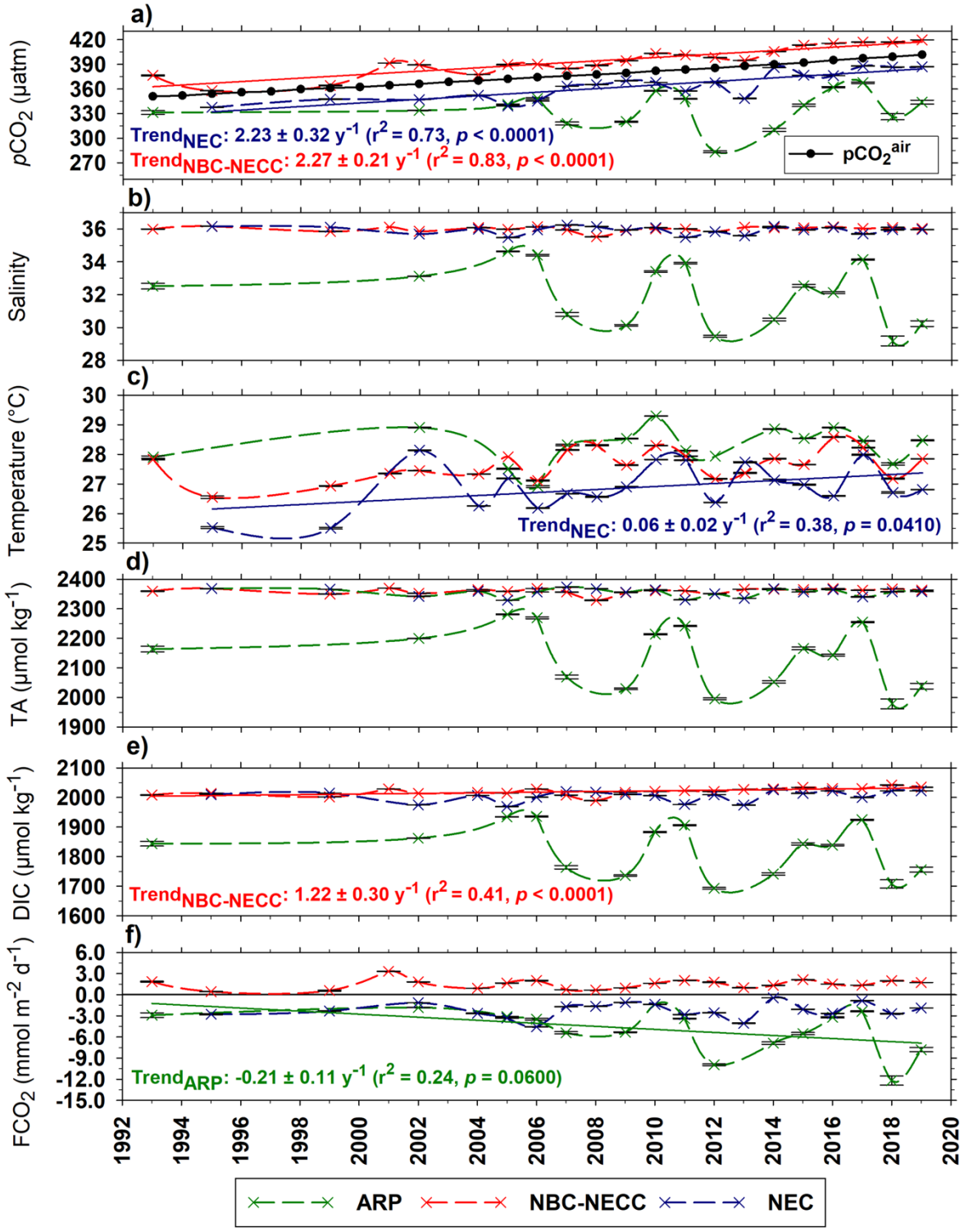

Figure 5: Time series of annual averages of **(a)** sea surface (colours) and atmospheric (black) CO_2 partial pressure (pCO_2), **(b)** salinity, **(c)** temperature, **(d)** total alkalinity (TA), **(e)** dissolved inorganic carbon (DIC) and **(f)** net sea-air CO_2 flux (FCO_2) in the Western Tropical Atlantic Ocean from 1993 to 2019. Three sub-regions are shown: North Brazil Current-North Equatorial Countercurrent – NBC-NECC (red), North Equatorial Current – NEC (blue), and the Amazon River plume – ARP (green). The dashed lines reflect the temporal trend of the parameters, and their colours are associated with the respective sub-regions. For significant trends (solid lines, with colour depicting sub-region), the trend ± standard deviation as well as its regression statistics are shown. The y-axis error bars (black) are the standard errors of the respective annual averages.

Accepted Article

This article is protected by copyright. All rights reserved.

4 Discussion

4.1 Main findings

We demonstrate that the western Tropical Atlantic Ocean can be split into three distinct sub-regions in terms of sea-air CO_2 exchanges. These contrasting behaviours of the three sub-regions explain why there is such inconsistency in estimates of sea-air CO_2 exchanges in this region (Table 1) since many of them are temporally and/or spatially restricted to the time of sampling. The sub-region under the NBC-NECC domain is a constant weak annual CO_2 source to the atmosphere, with minor interannual variability. This sub-region is limited by the ARP at approximately 50°W and by the NEC south of 10°N. The NEC sub-region acts as an annual CO_2 sink with greater temporal variability in CO_2 flux than the NBC-NECC sub-region. The Amazon River waters exert a great influence on the spatial variability of sea-air CO_2 exchanges in these two sub-regions. The ARP is the sub-region with the greatest interannual variability in CO_2 fluxes, but it acts as a persistent net oceanic sink for atmospheric CO_2. The CO_2 uptake is twice as high in the ARP core (i.e., SSS < 34), where the influence of the fresh and nutrient-enriched waters from the Amazon River is even greater than in its surroundings. Several processes act simultaneously to control the CO_2 system in the whole region. However, freshwater discharge seems to exert a strong influence on sea surface pCO_2 in the ARP domain, mainly through dilution and biological activity that is enhanced by riverine nutrient inputs. On the other hand, in the NBC-NECC and NEC domains sea-air CO_2 exchange is likely to be the dominant process. Despite the contrasting behaviour among the sub-regions, the entire region acted as a net annual CO_2 sink of -1.6 ± 1.0 mmol m^{-2} day^{-1} from 1993 to 2019. We also found a significant increasing trend in sea surface pCO_2 in NBC-NECC and NEC between 1993 and 2019, which is more pronounced than the increase in atmospheric pCO_2, revealing the sensitivity of carbon dynamics in these sub-regions to ongoing and expected changes in the global climate system.

This article is protected by copyright. All rights reserved.

Accepted Article

Table 1: Contrasting magnitudes of net sea-air CO_2 fluxes (FCO_2) recorded in the whole western Tropical Atlantic Ocean as well as in the different sub-regions such as North Brazil Current-North Equatorial Countercurrent (NBC-NECC), North Equatorial Current (NEC) – split by the climatology equilibrium isoline of annual averaged FCO_2 in the region, and Amazon River plume (ARP) – SSS < 35. Positive FCO_2 values indicate the outgassing of CO_2 to the atmosphere, whereas negative FCO_2 values indicate CO_2 uptake by the ocean. In the third column are shown the parameterizations used in the FCO_2 calculations (i.e., Wanninkhof, (1992) (W92); Wanninkhof & McGillis, (1999) (WM99); Sweeney et al., (2007) (S07); Wanninkhof, (2014) (W14) as well as the measure of wind speed used.

References	Temporal coverage	K_t Wind speed	Region domain Latitude; Longitude	**Region** Period	FCO_2 (mmol m^{-2} day^{-1})
This Study	Annual	W14 ERA5 reanalysis	5°S–15°N; 60°W–30°W	**Whole region** 1993-2019	–1.1 ± 1.6
				ARP 1993-2019	–5.0 ± 3.0
				NBC-NECC 1993-2019	1.5 ± 0.7
				NEC 1993-2019	–2.2 ± 1.0
Körtzinger, (2003)	Monthly	W92 Climatology	3°S–18°N; 30°W–60°W	**Whole region** October/November 2002	–1.4 ± 0.5
Cooley et al. (2007)	Monthly	WM99 Climatology	6°N–13°N; 48°W–58°W	**Whole region** 1995-1996, 2001-2003	1.4 ± 0.6
Lefèvre et al. (2010)	Annual	S07 Scatterometer	5°S–10°N; 65°W–35°W	**Whole region** 2006-2008	–1.0 ± 1.2
Ibánhez et al. (2015)	Annual	S07 ERA-interim reanalysis	5°N–14°N; 41°W–52°W	**Whole region** 2006-2013	–0.6 ± 6.1
Valerio et al. (2021)	Annual	W14 ECMWF product	5°S–15°N; 45°W–60°W	**Whole region** 2011-2014	4.6 ± 2.5
Carvalho et al. (2017)	Monthly	W14 *In situ*/ECMWF product	3°S–5°S; 35.5°W–38.5°W	**NBC-NECC** October 2012	3.3 ± 1.1
			1°S–4°S; 37°W–43°W	**NBC-NECC** September 2014	5.9 ± 3.1
Araujo et al. (2017)	Monthly	S07 Scatterometer	0°–8°N; 37°W–51°W	**NBC-NECC** October 2012	1.6 ± 3.4

Accepted Article

This article is protected by copyright. All rights reserved.

Araujo et al. (2018)*	Monthly	W14 *In situ*	15ºS–5ºN; 30°W–51ºW	**NBC-NECC** 1995-2001	0.3 ±1.7
Lefèvre et al. (2020)	Monthly	S07 ERA5	8°N; 38°W	**NBC-NECC** June-September 2013	0.6 ± 0.5
Mu et al. (2021)	Monthly	S07 *In situ/* ERA-interim reanalysis	0°–13°N; 45°W–60°W	**Whole region** September 2011	–0.4 ± 0.8
				ARP June 2010	–2.4 ± 1.3
				ARP/NBC-NECC July 2012	0.3 ± 0.6
Louchard et al. (2021)	Annual	Uninformed ERA-Interim reanalysis	0.5°–24°N; 30°W–70°W	**Whole region** 1998-2018	0.5
				ARP** 1998-2018	–0.9

*In this study sea surface pCO_2 was estimated from SST and SSS.
**For Louchard et al. (2021) the area of the ARP (~1.1 x 10^6 km^{-2}) was estimated at 12% of the total area of the Western Tropical Atlantic (9.6 x 10^6 km^{-2}) for the FCO_2 calculation.

Accepted Article

This article is protected by copyright. All rights reserved.

4.2 Regional variability and main drivers of sea-air CO_2 exchanges

4.2.1 Sea-air CO_2 exchanges in the North Brazil Current-North Equatorial Countercurrent

The sub-region under strong NBC-NECC dominance extends to approximately 50°W, where it is bounded by the waters from the Amazon River and is limited to south of 10°N by an isoline of equilibrium sea-air CO_2 exchanges. This sub-region is homogeneously a CO_2 source to the atmosphere throughout the year, which becomes more intense near the Brazilian coast, where the NBC flow is intensified (e.g., Johns et al., 1998; Salisbury et al., 2011). Such CO_2 outgassing behaviour is associated with warmer tropical waters (Fig. S6) (Azar et al., 2020; Johns et al., 2021) coupled with equatorial upwelling (Landschützer et al., 2014; Takahashi et al., 2009). Moreover, the influence of CO_2-enriched waters from the Indian Ocean (Orselli et al., 2019a, b), which are advected by mesoscale structures along the South Atlantic Ocean (Souza et al., 2018; Azar et al., 2021), may strengthen the seawater CO_2 supersaturation in this sub-region. During the wet season, there is a greater influence of the waters from the Amazon River over the western Tropical Atlantic Ocean (Lefèvre et al., 2020; Louchard et al., 2021; Mu et al., 2021). This is coupled with increased precipitation due to the northward displacement of the ITCZ (Ibánhez et al., 2015; Utida et al., 2019), hence leading to a net pCO_2 drawdown in the NBC-NECC sub-region, although it remains supersaturated with respect to atmospheric pCO_2. The decrease in DIC and SSS (Fig. 3b) suggests that the pCO_2 drawdown is mainly driven by the physical solubility pump, which has already been suggested as the main driver of pCO_2 changes in this sub-region (Araujo et al., 2018). This is more evident when TA and DIC are normalised to SSS, revealing that pCO_2 drawdown is almost counteracted by the increase in SST, which decreases the CO_2 solubility. This occurs mainly in the NBC-NECC core, where surface waters are typically warmer (Fig. S6) (Johns et al., 1998; Salisbury et al., 2011) and the CO_2 release is doubled near the Brazilian coast (Fig. 2). In addition, NBC-NECC is a favourable sub-region for calcium carbonate precipitation (Fig. 4), allowing the

This article is protected by copyright. All rights reserved.

Accepted Article

development of the extensive reef system at the Amazon River mouth (Moura et al., 2016; Francini-Filho et al., 2018; Neumann-Leitão et al., 2018).

4.2.2 Sea-air CO_2 exchanges in the North Equatorial Current

The NEC sub-region is a moderate CO_2 sink, but with greater internal variability than NBC-NECC. This is evidenced by higher spatial heterogeneity in the sea-air CO_2 flux in the NEC sub-region, which is intensified to the northwest where the influence of waters from the Amazon River is greater. In fact, the waters from the Amazon River are expected to have influence on the position of the sea-air CO_2 equilibrium isoline that demarcates the NEC and NBC-NECC sub-regions, due to the NBC retroflection transporting riverine waters in the wet season (Garzoli et al., 2004; Goes et al., 2005; Lefèvre et al., 2020). However, the increase in sea surface pCO_2 driven by the increase in DIC during the wet season (Fig. 3) indicates that the influence of NBC-NECC waters supersaturated in CO_2 overlaps with the influence of Amazon River waters in this period. Furthermore, this increase in pCO_2 may be associated with the influence of CO_2-rich waters from the Canary upwelling system (Landschützer et al., 2020), which influences the NEC before reaching the western tropical Atlantic (Ibánhez et al., 2017). This leads to a net increase in pCO_2 over the whole NEC (Fig. 3) during maximum NBC retroflection, despite the nutrient- and carbon-enriched waters from the Amazon River (Lefèvre et al., 2020). During the dry season, instead of being transported to the east, the waters from the Amazon River are mainly advected to the northwest, decreasing pCO_2 in the NEC sub-region due to high primary productivity (Bonou et al., 2016; Ibánhez et al., 2015; Mu et al., 2021; Louchard et al., 2021), hence intensifying the biological uptake of CO_2 (Fig 2a). Indeed, model estimates suggested that without the influence of the Amazon River, much of the western Tropical Atlantic Ocean, including part of the NEC sub-region, would be a CO_2 source year-round (Louchard et al., 2021). Nevertheless, CO_2 uptake is reduced east of the NEC sub-region, where sea-air CO_2 exchange is close to ocean-atmosphere equilibrium (Fig. 2c). It is a note of

This article is protected by copyright. All rights reserved.

Accepted Article

mention that previous studies have recorded a CO_2 release during the wet season in the NEC sub-region (Lefèvre et al., 2014; Ibánhez et al., 2015; Ibánhez et al., 2017). These records were associated with the influence of extreme events driven by ENSO (i.e., 2009 and 2010), leading to anomalous SST and consequent increase in sea surface pCO_2. We also observed these signs of CO_2 release in 2009, 2010 and 2014 (Fig. S3), but further investigations are needed to assess to what extent this behaviour should be considered anomalous as well as its periodicity, which might also be associated with the influence of the Canary upwelling system (Landschützer et al., 2020). Although the ITCZ lies to the north during most of the wet season (Utida et al., 2019), precipitation does not seem to exert a strong influence on pCO_2 seasonality in the NEC. Otherwise, the increase in pCO_2 would be partially attenuated, due to the dilution process (Ho & Schanze, 2020), and SSS would decrease rather than increase during the wet season (Fig. 3b). This suggests that the hydrographic and biogeochemical properties in the NEC vary with ocean circulation (e.g., Bruto et al., 2017) rather than precipitation. Thus, the seasonal changes in pCO_2, and hence in sea-air CO_2 exchanges, in NEC are likely driven by CO_2 release and uptake processes controlled by the variability of ocean dynamics and to some extent by the Canary upwelling system.

4.2.3 Sea-air CO_2 exchanges in the Amazon River plume

The ARP is the most complex sub-region for understanding the changes in the marine carbonate system, since several processes act together, with often contrasting influences on sea surface pCO_2. The strength of each of these processes is likely coupled with the balance between freshwater discharge and seawater influence since there was a great difference in sea surface pCO_2 drivers after normalisation to SSS. For instance, sea surface pCO_2 drawdown in the wet season (Fig. 3) is driven by the dilution of riverine waters through mixing with seawater (Bonou et al., 2016; Varona et al., 2018; Mu et al., 2021; Louchard et al., 2021). In addition, the calcium carbonate calcification and dissolution processes are also intensified as SSS

This article is protected by copyright. All rights reserved.

increases (Fig. 4c), although their net effect on sea surface pCO_2 is not clear. Moreover, the pronounced sea surface pCO_2 drawdown in the wet season is also due to the uptake of CO_2 during phytoplankton growth, mainly diatoms and diatom-diazotroph-assemblages (Louchard et al., 2021), driven by nutrient enrichment from Amazon River waters (Smith & Demaster, 1996; Dagg et al., 2004; da Cunha & Buitenhuis, 2013; Louchard et al., 2021). Although the relative influence of each of these processes (i.e., dilution and photosynthesis) on pCO_2 remains unclear, most studies conducted in the ARP sub-region indicate that biological activity is the main driver for the sea surface pCO_2 drawdown (Kortzinger, 2003; Bonou et al., 2016; Lefèvre et al., 2017; Mu et al., 2021; Louchard et al., 2021). However, we identified a decrease in TA in the wet season (Fig. 3a), rather than a small increase expected as a result of photosynthesis, revealing the influence of TA dilution through mixing of marine and riverine waters (Bonou et al., 2016; Araujo et al., 2018; Louchard et al., 2021). Furthermore, the increase only in normalised DIC (Fig. 3b) reveals the influence of carbon remineralised from particulate and dissolved organic matter, transported by the waters of the Amazon River during the wet season (Ward et al., 2013; Mu et al., 2021; Louchard et al., 2021). Thus, both the increase in DIC from remineralisation and the decrease in TA from dilution lead to an increase in sea surface pCO_2, but this is not sufficient to counteract the pCO_2 drawdown by primary production. Therefore, photosynthesis is the main driver of sea surface pCO_2 drawdown in the ARP (Fig. S8), as has been suggested in a number of previous studies (Kortzinger, 2003; Bonou et al., 2016; Lefèvre et al., 2017; Mu et al., 2021; Louchard et al., 2021). Moreover, both CO_2 solubility and calcium carbonate dissolution by riverine waters likely exert some influence on the marine carbonate system. This may have some effect on the extent of the reef system, as it appears to be limited to the warmer and more saline waters under the NBC-NECC domain (e.g., Moura et al., 2016; Francini-Filho et al., 2018; Neumann-Leitão et al., 2018). The annual average net CO_2 flux across the whole region drops considerably from –1.6 to –0.2 mmol m^{-2} day^{-1}, when we remove

This article is protected by copyright. All rights reserved.

the ARP sub-region. Thus, the waters derived from ARP are responsible for 87% of the CO_2 uptake by the western Tropical Atlantic Ocean, a greater contribution than the 60% showed by biogeochemical models (Louchard et al., 2021). Hence, further observational efforts are needed to broaden our understanding of this biogeochemically complex region, and thus to improve ocean and climate model estimates.

4.3 Temporal variability and trends in sea-air CO_2 exchanges

The progressive increase in sea surface pCO_2 is likely associated mainly with the increase in SST in both NEC and NBC-NECC waters and DIC in the NBC-NECC domain (Fig. 5c, e). For instance, the sea surface pCO_2 growth trend decreased by 35% in NEC and by 31% in NBC-NECC waters when we removed its thermal effect (Fig. 6). Indeed, an increase in SST has been reported in the North Atlantic (Bates & Johnson, 2020), where NEC waters originate before being advected to the Tropical Atlantic (e.g., Lefèvre et al., 2014). The NBC-NECC sub-region is influenced by both CO_2-rich waters from the equatorial upwelling (e.g., Lefèvre et al., 2014) and warmer, more saline upper waters from the South Atlantic Ocean. Those waters comprise a considerable contribution (34%) derived from the Indian Ocean, which are transported through the Agulhas eddies along the South Atlantic Ocean (Souza et al., 2018; Azar et al., 2021). In fact, around 20% of those waters that reach the NBC system through the southern South Equatorial Current bifurcation is sourced from the Indian Ocean (Azar et al., 2021). Thus, the mesoscale activity along the South Atlantic Ocean likely acts as an interhemispheric coupling component also influencing the CO_2 behaviour in the NBC-NECC sub-region through the transfer of biogeochemical properties between ocean basins (Orselli et al., 2019a, 2019b). For instance, the Agulhas eddies typically intensify the ocean CO_2 uptake along their pathway in the South Atlantic (Orselli et al., 2019a), increasing their initial DIC storage from Indian

This article is protected by copyright. All rights reserved.

Ocean waters. Hence, those structures also contain more anthropogenic carbon than the surrounding waters (Orselli et al., 2019b). Since the release of the Agulhas eddies has been intensifying (Biastoch et al., 2009; Lübbecke et al., 2015), it is likely that part of the increase in DIC and sea surface pCO_2 in the NBC-NECC domain is explained by the increasing influence of these waters being transferred to the NBC current system.

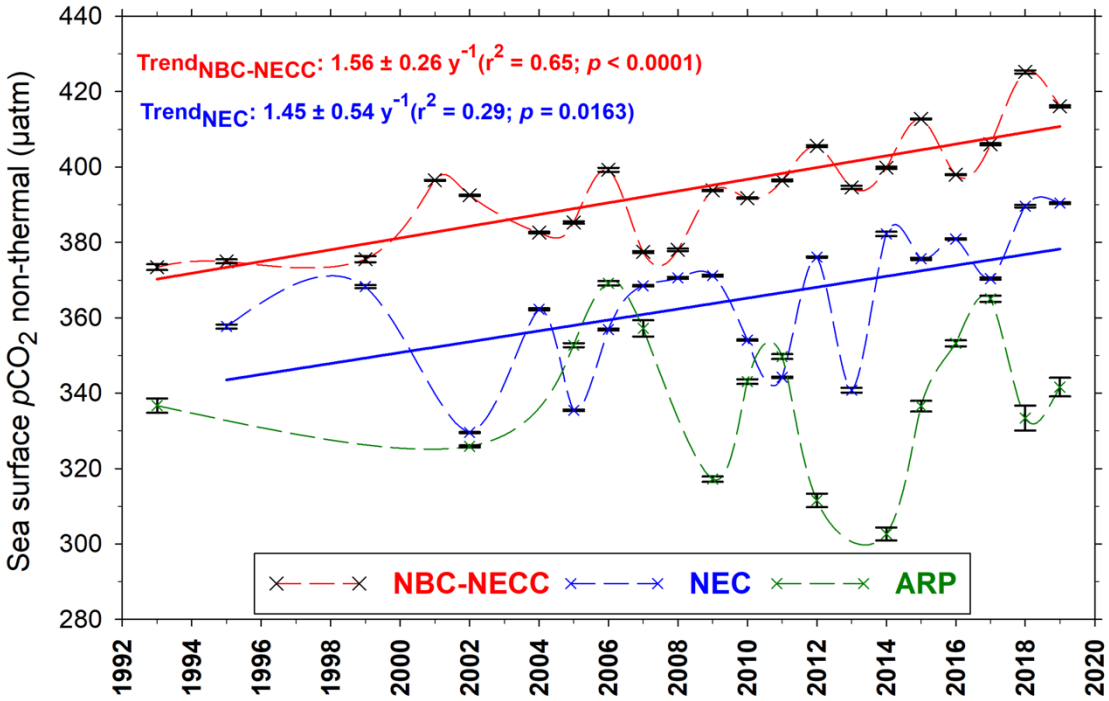

Figure 6: Time series of annual averages of sea surface CO_2 partial pressure normalised to annual average surface temperature in North Brazil Current-North Equatorial Countercurrent – NBC-NECC (red), North Equatorial Current – NEC (blue), and Amazon River plume – ARP (green) sub-regions. For significant trends (solid lines, with colour depicting sub-region), the trend ± standard deviation as well as their regression statistics are shown. The y-axis error bars (black) are the standard errors of the respective annual averages.

A sea surface pCO_2 increase of 1.20 ± 0.02 µatm year^{-1} in the NBC-NECC sub-region was reported for 1983-2010, but was lower than the increase in atmospheric pCO_2 of 1.70 µatm year^{-1} over the same period (Araujo et al., 2018). This trend in sea surface pCO_2 has increased rapidly to the current estimate of 2.27 ± 0.21 µatm year^{-1} from 1993 to 2019 (Fig. 5a), indicating that it is likely to continue to accelerate in the coming years. This is also observed in the NEC sub-region (Fig. 5a), as it is influenced by the circulation and ocean dynamics of the NBC-NECC system (Garzoli et al., 2004; Goes et al., 2005; Varona et al., 2018; Lefèvre et

This article is protected by copyright. All rights reserved.

al., 2020). In fact, Park & Wanninkhof (2012) identified a sea surface pCO_2 growth rate (0.17 ± 1.23 µatm year^{-1}) north of 18°N that was lower than atmospheric pCO_2 growth (2.05 ± 0.09 µatm year^{-1}) until 2009, mainly during the boreal winter (dry season). However, they identified a higher sea surface pCO_2 growth (1.57 ± 0.86 µatm year^{-1}) in boreal summer (wet season), which is in agreement with our findings of higher sea surface pCO_2 growth during the wet season (Fig. S5). Furthermore, the sea surface pCO_2 growth in NEC has intensified from 2009, as well as in the NBC-NECC sub-region. In both sub-regions, the rate of increase in sea surface pCO_2 is greater than that of atmospheric pCO_2 (1.93 ± 0.02 µatm year^{-1}; $p < 0.0001$). Therefore, CO_2 outgassing is intensifying in the NBC-NECC while the NEC sub-region can be expected to show a trend towards CO_2 equilibrium with the atmosphere.

Assuming a growth in atmospheric pCO_2 at current levels (1.93 µatm year^{-1}), these trends suggest that it will take around 50 years for sea surface pCO_2 in the NEC to reach equilibrium with atmospheric pCO_2 and from there begin predominantly releasing CO_2. At the same time, the disequilibrium between sea-air CO_2 in NBC-NECC is expected to double, intensifying the CO_2 outgassing. Indeed, although this sub-region is relatively resilient to decreased seawater buffering capacity (Jiang et al., 2019), we observed a small yet significant increasing trend in Revelle Factor (Fig. S7), indicating a likely reduction in buffering capacity in both NEC and NBC-NECC waters. However, since this trend in sea surface pCO_2 in NBC-NECC increased rapidly by 33% from 2010 to 2019, it is likely that this equilibrium point in NEC and intensification in NBC-NECC will be reached even before the 50 years projected based on a linear increase in atmospheric pCO_2. The timing of these changes will depend on global CO_2 emissions and the future evolution of atmospheric pCO_2 in the coming years, as reflected in the Shared Socioeconomic Pathways (SSP) (Meinshausen et al., 2020) used in the latest IPCC report (IPCC, 2021). For instance, if global CO_2 emissions are cut to net zero by around 2050, in the most optimistic scenario (SSP1-1.9), the NEC sub-region would switch to releasing

This article is protected by copyright. All rights reserved.

Accepted Article

instead of taking up CO_2 and NBC-NECC would double its CO_2 outgassing in approximately 20 years, assuming the current sea surface pCO_2 trend. However, it remains difficult to predict an accurate response of the marine carbonate system to different scenarios, because sea-air CO_2 exchanges are an important driver for sea surface pCO_2 in these sub-regions (e.g., Araujo et al., 2018). In any case, the increase in sea surface pCO_2 can further lead to changes in seawater pH and hence affect the extensive reef system at the Amazon River mouth along the continental shelf (Moura et al., 2016), which is highly sensitive to changes in biogeochemical conditions (Francini-Filho et al., 2018; Neumann-Leitão et al., 2018).

The ARP sub-region exhibits high interannual variability but no trend in sea surface pCO_2. However, there is a trend (at the 94% confidence level) towards an increase in CO_2 uptake in this sub-region (Fig. 5f) because of the increase in atmospheric pCO_2 (Fig. 5a) and therefore the sea-air CO_2 disequilibrium. The Amazon River plume waters have been experiencing an increasing trend in the concentration of chlorophyll-a from 1997 to 2020 (Fig. S8), which is likely associated with the amplification of the hydrological cycle in this sub-region (Liang et al., 2020), characterised by an increase in precipitation and discharge from the Amazon River. The waters exported from the Amazon River are the main source of nutrients that enrich the ARP sub-region for phytoplankton growth (Bonou et al., 2016; Ibánhez et al., 2015; Mu et al., 2021; Louchard et al., 2021). Hence, the increasing trend in ARP sea surface pCO_2 expected due to both the increase in atmospheric pCO_2 and sea surface pCO_2 in the surroundings is completely counteracted by the increase in biological CO_2 uptake. The strong interannual variability of the carbonate system in the ARP sub-region is matched by the variability in SSS (Fig. 5). However, it remains unclear which is the main driver of this strong interannual variability, since several processes act together and decomposing them is still a challenge (Bonou et al., 2016; Ibánhez et al., 2015; Mu et al., 2021; Louchard et al., 2021; Valerio et al., 2020). For example, although precipitation driven by the ITCZ position intensifies in the wet

This article is protected by copyright. All rights reserved.

Accepted Article

season south of 10°N, it has not been associated with interannual pCO_2 variability in this sub-region (Lefèvre et al., 2020). Nevertheless, the years with the highest SSS and pCO_2 (2005, 2010 and 2011) were those with the most significant droughts due to the coupled influence of the El Niño phase of ENSO with warming of the tropical North Atlantic (Marengo & Espinoza, 2016; Tyaquiçã et al., 2017). Conversely, the lowest SSS and pCO_2 were found in years (2009 and 2012-2014) marked by heavy flooding associated with the La Niña phase and warming of the tropical South Atlantic (Marengo & Espinoza, 2016; Tyaquiçã et al., 2017). Such climatic events add complexity to the dynamics of the carbon cycle in the western Tropical Atlantic Ocean (Kucharski et al., 2016) and require further investigation using observations, models (Louchard et al., 2021), reanalysis products and satellite imagery (e.g., Valerio et al., 2021; Liutti et al., 2021) to constrain their relative importance to regional biogeochemistry.

5 Caveats and limitations

Although the contrasting behaviour of sea-air CO_2 exchanges in the sub-regions of the western Tropical Atlantic is evident, the marine carbonate system sampling is limited before the 2000s. As such, the increasing trends in sea surface pCO_2 may be even greater than those we found here. However, this limits us to associating the inter-annual variability of sea surface pCO_2 in the ARP sub-region with its likely drivers, such as precipitation, river discharge and chlorophyll-a concentrations (Fig. S1). Despite our findings suggesting that the behaviour of the NBC-NECC, NEC and ARP sub-regions is consistent in the dry and wet seasons in terms of average FCO_2, our time series is limited to just one season in some years, mainly until 2009 (Fig. S2). Nevertheless, the CO_2 source or CO_2 sink behaviour in each sub-region is evident in the years in which there is sampling in both dry and wet seasons (Fig. S3). The ARP is the sub-region with the lowest spatial and temporal data coverage. Although temporal coverage has increased since 2006, when both dry and wet season data are available more frequently, the temporal variability of the average annual pCO_2 in the ARP may be biased by the greater

This article is protected by copyright. All rights reserved.

Accepted Article

amount of data in the wet season (Fig. S5). This demonstrates that the ARP is a priority sub-region to focus efforts on future studies to solve the issue of seasonal biases in data coverage.

Another complication is that organic substances influence alkalinity measurements, mainly in estuarine waters (e.g., Kerr et al, 2021). Moreover, although the organic fraction of alkalinity over a vast area of the western Tropical Atlantic Ocean is estimated to be less than 5 µmol kg^{-1} (Kerr et al, 2021), this fraction may be higher in ARP waters, because of riverine transport. Since the TA that we estimated from SSS, SST and location (Carter et al., 2018) does not consider the organic fraction of alkalinity, the TA may be underestimated, and this could influence the TA:DIC ratios to some extent. This may be an explanation for the lack of a clearly observed increase in TA as a result of photosynthesis (Fig. 4c). In fact, the organic fraction in TA has been a global challenge in studies of the carbonate system in coastal regions (Kerr et al, 2021) and a limitation shared among several studies conducted to date in the western tropical Atlantic Ocean (e.g., Kortzinger, 2003; Lefèvre et al., 2010; Araujo et al., 2014; Lefèvre et al., 2014; Bonou et al., 2016; Araujo et al., 2017; Lefèvre et al., 2017; Araujo et al., 2018). Furthermore, other biogeochemical aspects need to be investigated in future studies to elucidate the consequences of the increase in sea surface pCO_2 in the NEC and NBC-NECC sub-regions, and what has been driving the resilience of the ARP to this increase. Since little is known about the temporal and spatial variability of the carbonate system properties in the whole region, separating the main processes driving the sea surface pCO_2 changes remains a challenge, as several processes act simultaneously.

6 Conclusions and closing remarks

The contrasting estimates in sea-air CO_2 exchanges in the western Tropical Atlantic Ocean occur because this region is composed of three distinct sub-regions in terms of these exchanges. The sub-region under the North Brazil Current domain is a net annual CO_2 source to the atmosphere, while the sub-region under the North Equatorial Current influence is a net annual

This article is protected by copyright. All rights reserved.

Accepted Article

CO_2 sink. The Amazon River plume waters are a strong net CO_2 sink, being responsible for 87% of the CO_2 uptake in the western Tropical Atlantic Ocean. Since several studies have only used snapshots of sea-air CO_2 exchanges in this region, the comprehensive approach of this study expands our knowledge about their spatial and temporal dynamics. Our findings shed light on the risk of extrapolation in estimating sea-air CO_2 exchanges from geographic or temporal snapshots. Hence, in addition to pointing out questions that still need to be answered on the marine carbonate system, our study may be useful for informing the sampling design of future studies in this region. Increased availability of observational data should significantly improve the performance of complex coupled models (e.g., ocean-biogeochemical and climate models) to provide more robust information about the natural behaviour and changes underway and anticipated in the western Tropical Atlantic Ocean. Finally, the significant increase in sea surface pCO_2 in both the North Brazil Current and North Equatorial Current reveals the sensitivity of carbon dynamics in these sub-regions to global climate change.

Acknowledgements

This study contributes to the activities of the Brazilian Ocean Acidification Network (BrOA; www.broa.furg.br) and the CARBON Team (www.carbonteam.furg.br). T.M. received financial support from the Brazilian Improving Coordination of Higher Education Personnel (CAPES, PhD Grant No. 88887.360799/2019-00), allowed by the PROVOCCAR project and sponsored by the Brazilian National Council for Scientific and Technological Development (CNPq) Grant No. 442628/2018-8; and from CNPq Grant No. 200649/2020-5 for an abroad PhD period supervised by S.H. R.K. received financial support from CNPq researcher Grant Nos. 304937/2018-5 and 309978/2021-1. M.A. thanks the Brazilian Research Network on Global Climate Change - Rede CLIMA (FINEP-CNPq 437167/2016-0) and the Brazilian National Institute of Science and Technology for Tropical Marine Environments - INCT AmbTropic (CNPq/FAPESB 565054/2010-4 and 8936/2011) for their support. We are thankful for the support provided by CAPES to the Graduate Program in Oceanology and the FURG project CAPES-PrInt. We appreciate the availability of high-quality data from the SOCAT (https://www.socat.info/), GLODAP (https://www.glodap.info/) and Barbados Station datasets https://gml.noaa.gov/dv/data/index.php?category=Greenhouse%2BGases&parameter_name=Carbon%2BDioxide&site=RPB). Special thanks to the scientists Dorothee Bakker, Wanninkhof, R.; Lefèvre, N.; Pierrot, D.; Ritschel, M; González-Dávila, M.; Santana-Casiano, J. M.; Goyet, C.; Gutekunst, S.; Ríos, A. F.; Schuster, U.; Tanhua, T.; Wallace, D. and Diverrès, D., who have made the invaluable surface ocean pCO_2 measurements publicly available via the

This article is protected by copyright. All rights reserved.

Accepted Article

SOCAT dataset. We thank Andrés Pinãngo for his help in obtaining and analysing satellite chlorophyll data.

Data Availability Statement

The data that support the findings of this study are published openly at: SOCAT (https://www.socat.info/), GLODAP (https://www.glodap.info/), Barbados Station datasets https://gml.noaa.gov/dv/data/index.php?category=Greenhouse%2BGases&parameter_name=Carbon%2BDioxide&site=RPB), ERA 5 reanalysis (https://cds.climate.copernicus.eu/cdsapp#!/dataset/reanalysis-era5-single-levels-monthly-means?tab=overview), Óbidos station (http://www.snirh.gov.br/hidrotelemetria/Mapa.aspx), and Ocean-Colour Climate Change Initiative project (https://climate.esa.int/en/projects/ocean-colour/).

References

Araujo, M., Noriega, C. E. D., Lefèvre, N. (2014). Nutrients and carbon fluxes in the estuaries of major rivers flowing into the tropical Atlantic. *Frontiers in Marine Science*, 1, 10. https://doi.org/10.3389/fmars.2014.00010.

Araujo, M., Noriega, C., Hounsou-Gbo, G. A., Veleda, D., Araujo, J., Bruto, L., et al. (2017). A Synoptic Assessment of the Amazon River-Ocean Continuum during Boreal Autumn: From Physics to Plankton Communities and Carbon Flux. *Frontiers in Microbiology*, 8, 1358. https://doi.org/10.3389/fmicb.2017.01358.

Araujo, M., Noriega, C., Medeiros, C., Lefèvre, N., Ibánhez, J. S. P., Montes, M. F., et al. (2018). On the variability in the CO2 system and water productivity in the western tropical Atlantic off North and Northeast Brazil. *Journal of Marine Systems*, 1, 1. https://doi.org/10.1016/j.jmarsys.2018.09.008.

Aroucha, L. C., Veleda, D., Lopes, F. S., Tyaquiçã, P., Lefèvre, N., & Araujo, M. (2020). Intra- and Inter- Annual Variability of North Brazil Current Rings Using Angular Momentum Eddy Detection and Tracking Algorithm: Observations From 1993 to 2016. *Journal of Geophysical Research: Oceans*, 125, 12. https://doi.org/10.1029/2019JC015921.

Azar, E., Piango, A., Wallner-Kersanach, M., & Kerr, R. (2020). Source waters contribution to the tropical Atlantic central layer: new insights on the Indo-Atlantic exchanges. *Deep Sea Research Part I: Oceanographic Research Papers*, 168, 103450. https://doi.org/10.1016/j.dsr.2020.103450.

Bakker, D. C. E. et al. (2016). A multi-decade record of high quality fCO_2 data in version 3 of the Surface Ocean CO_2 Atlas (SOCAT). *Earth System Science Data*, 8, 2, 383– 413. https://doi.org/10.5194/essd-8-383-2016.

Bates, N. R., & Johnson, R. J. (2020). Acceleration of ocean warming, salinification, deoxygenation and acidification in the surface subtropical North Atlantic Ocean. *Communications Earth & Environment*, 1, 33. https://doi.org/10.1038/s43247-020-00030-5.

This article is protected by copyright. All rights reserved.

Accepted Article

Biastoch, A., Beal, L., Lutjeharms, J., & Casal, T. 2009. Variability and coherence of the Agulhas Undercurrent in a high-resolution ocean general circulation model. *Journal of Physical Oceanography*, 39, 10, 2417–2435. https://doi.org/10.1175/2009JPO4184.1.

Bonou, F. K., Noriega, C., Lefèvre, N., & Araujo, M. (2016). Distribution of CO_2 parameters in the Western Tropical Atlantic Ocean. *Dynamics of Atmospheres and Oceans*, 73, 47–60. https://doi.org/10.1016/j.dynatmoce.2015.12.001.

Bruto, L., Araujo, M., Noriega, C., Veleda, D., & Lefèvre, N. (2017). Variability of CO_2 fugacity at the western edge of the tropical Atlantic Ocean from the 8°N to 38°W PIRATA buoy. *Dynamics of Atmospheres and Oceans*, 78, 12017. https://doi.org/10.1016/j.dynatmoce.2017.01.003.

Cai, W. J., & Wang, Y. (1998). The chemistry, fluxes, and sources of carbon dioxide in the estuarine waters of the Satilla and Altamaha Rivers, Georgia. *Limnology and Oceanography*, 43(4), 657-668. https://doi.org/10.4319/lo.1998.43.4.0657.

Carter, B. R., Feely, R. A., Williams, N. L., Dickson, A. G., Fong, M. B., & Takeshita, Y. (2018). Updated methods for global locally interpolated estimation of alkalinity, pH, and nitrate. *Limnology and Oceanography: Methods*, 16, 2, 119–131. https://doi.org/10.1002/lom3.10232.

Carvalho, A. C. O., Marins, R. V., Dias, F. J. S., Rezende, C. E., Lefèvre, N., Cavalcante, M. S., et al. (2017). Air-sea CO2 fluxes for the Brazilian northeast continental shelf in a climatic transition region. *Journal of Marine Systems*, 173, 70–80. https://doi.org/10.1016/j.jmarsys.2017.04.009.

Coles, V. J., Brooks, M. T., Hopkins, J., Stukel, M. R., Yager, P. L., & Hood, R. R. (2013), The pathways and properties of the Amazon River plume in the tropical North Atlantic Ocean. *Journal of Geophysical Research: Oceans*, 118, 6894– 6913. https://doi.org/10.1002/2013JC008981.

Cooley, S.R., Coles, V.J., Subramaniam, A., Yager, P.L. (2007). Seasonal variations in the Amazon plume-related atmospheric carbon sink. *Global Biogeochemical Cycles*, 21, 1–15, http://doi.org/10.1029/2006GB002831.

Da Cunha, L. C., & Buitenhuis, E. T. (2013). Riverine influence on the tropical Atlantic Ocean biogeochemistry. *Biogeosciences*, 10, 10, 6357–6373. https://doi.org/10.5194/bg-10-6357-2013.

Dagg, M., Benner, R., Lohrenz, S., & Lawrence, D. (2004). Transformation of dissolved and particulate materials on continental shelves influenced by large rivers: Plume processes. *Continental Shelf Research*, 24, 7–8, 833–858. https://doi.org/10.1016/j.csr.2004.02.003.

Dickson, A. G. (1990). Standard potential of the reaction: AgCl(s) + 1/2H2(g) = Ag(s) + HCl(aq), and the standard acidity constant of the ion HSO4 - in synthetic sea water from 273.15 to 318.15 K. *The Journal of Chemical Thermodynamics*, 22, 2, 113–127. https://doi.org/10.1016/0021-9614(90)90074-Z.

Dickson, A. G., & F. J. Millero (1987), A comparison of the equilibrium constants for the dissociation of carbonic acid in seawater media, *Deep Sea Research Part A. Oceanographic Research Papers*, 34, 1733– 1743. https://doi.org/10.1016/0198-0149(87)90021-5.

This article is protected by copyright. All rights reserved.

Accepted Article

Didden, N. and F. Schott. (1993). Eddies in the North Brazil Current retroflection region observed by Geosat altimetry. *Journal of Geophysical Research: Oceans*, 98, C11, 20121-20131. https://doi.org/10.1029/93JC01184.

Dlugokencky, E.J., Mund, J.W., Crotwell, A.M., Crotwell, M.J., & Thoning, K.W. (2021), Atmospheric Carbon Dioxide Dry Air Mole Fractions from the NOAA GML Carbon Cycle Cooperative Global Air Sampling Network, 1968-2020, Version: 2021-07-30. https://doi.org/10.15138/wkgj-f215.

Fonseca, C. A., Campos, E., Goni, G.J., Johns, W.E. (2004). Investigation of the North Brazil Current retroflection and North Equatorial Countercurrent variability. *Geophysical Research Letters*, 31, 1-5. https://doi.org/10.1029/2004GL020054.

Francini-Filho, R., Asp, N. E., Siegle, E., Hocevar, J., Lowyck, K., D'Avila, N., et al. (2018). Perspectives on the Great Amazon Reef: Extension, biodiversity, and threats. *Frontiers in Marine Science*, 5, 142. https://doi.org/10.3389/fmars.2018.00142.

Friedlingstein, P., O'Sullivan, M., Jones, M.W., Andrew, R.M., Hauck, J., Olsen, A., et al. (2020). Global carbon budget 2020. *Earth System Science Data*, 12, 3269– 3340. https://doi.org/10.5194/essd-12-3269-2020.

Friis, K., Körtzinger, A., & Wallace, D. W. R. (2003). The salinity normalization of marine inorganic carbon chemistry data. *Geophysical Research Letters*, 30, 2, 1085. https://doi.org/10.1029/2002GL015898.

Garzoli, S.L., Ffield, A., Johns, W.E., Yao, Q. (2004). North Brazil Current retroflection and transports. *Journal of Geophysical Research*, 109, 1–13. http://dx.doi.org/10.1029/2003JC001775.

Gaube, P., McGillicuddy, D. J., Chelton, D. B., Behrenfeld, M. J., & Strutton, P. G. (2014). Regional variations in the influence of mesoscale eddies on near-surface chlorophyll. *Journal of Geophysical Research: Oceans*, 119, 12, 8195–8220. https://doi.org/10.1002/2014JC010111.

Goes, M., Molinari, R., Silveira, I., Wainer, I. (2005). Retroflections of the North Brazil Current during February 2002. *Deep Sea Research Part I: Oceanographic Research Papers*, 52, 647–667. https://doi.org/10.1016/j.dsr.2004.10.010.

Hellweger F., & Gordon, A. (2002). Tracing Amazon River water into the Caribbean Sea. *Journal of Marine Research*, 60, 537–549. https://doi.org/10.1357/002224002762324202.

Hersbach, H., Bell, B., Berrisford, P. et al. (2020). The ERA5 global reanalysis. *Quarterly Journal of the Royal Meteorological Society*,146, 1999–2049. https://doi.org/10.1002/qj.3803.

Ho, D. T., & Schanze, J. J. (2020). Precipitation- Induced Reduction in Surface Ocean pCO2: Observations from the Eastern Tropical Pacific Ocean. *Geophysical Research Letters*, *47*, 15. https://doi.org/10.1029/2020GL088252.

This article is protected by copyright. All rights reserved.

Accepted Article

Ibánhez, J. S., Diverrès, D., Araujo, M. & Lefèvre, N. (2015). Seasonal and interannual variability of sea-air CO2 fluxes in the tropical Atlantic affected by the Amazon River plume. *Global Biogeochemical Cycles*, 29, 10, 1640-1655. https://doi.org/10.1002/2015GB005110.

Ibánhez, J. S., Araujo, M. & Lefèvre, N. (2016). The overlooked tropical oceanic CO2 sink. *Geophysical Research Letters*, 43, 8, 3804-3812. https://doi.org/10.1002/2016GL068020.

Ibánhez, J., Flores, M. & Lefèvre, N. (2017). Collapse of the tropical and subtropical North Atlantic CO_2 sink in boreal spring of 2010. *Scientific Reports*, 7, 41694. https://doi.org/10.1038/srep41694.

IPCC, 2021: Climate Change 2021: The Physical Science Basis. Contribution of Working Group I to the Sixth Assessment Report of the Intergovernmental Panel on Climate Change [Masson-Delmotte, V., P. Zhai, A. Pirani, S. L. Connors, C. Péan, S. Berger, N. Caud, Y. Chen, L. Goldfarb, M. I. Gomis, M. Huang, K. Leitzell, E. Lonnoy, J. B. R. Matthews, T. K. Maycock, T. Waterfield, O. Yelekçi, R. Yu, and B. Zhou (eds.)]. Cambridge University Press. In Press.

Jiang, L. Q. et al. (2019). Surface ocean pH and buffer capacity: past, present and future. *Scientific Reports* 9, 18624. https://doi.org/10.1038/s41598-019-55039-4.

Johns, W. E., Lee, T., Beardsley, R. C., Candela, J., Limeburner, R., & Castro B. M. (1998). Annual cycle and variability of the North Brazil Current. *Journal of Physical Oceanography*, 28, 103–128. https://doi.org/10.1175/1520-0485(1998)028<0103:ACAVOT>2.0.CO;2.

Johns, William, S. Speich, M. Araujo et al. (2021). Tropical Atlantic Observing System (TAOS) Review Report. *CLIVAR-01/202*1, 218. https://archimer.ifremer.fr/doc/00696/80787/.

Kerr, D. E., Brown, P. J., Grey, A., Kelleher, B. P. The Influence of Organic Alkalinity on the Carbonate System in Coastal Waters. Mar. Chem. 2021, 104050. DOI: 10.1016/j.marchem.2021.104050.

Korosov, A., Counillon, F., Johannessen, J. A. (2015). Monitoring the spreading of the Amazon freshwater plume by MODIS, SMOS, Aquarius, and TOPAZ. *Journal of Geophysical Research: Oceans*, 120, 268–283. https://doi.org/10.1002/2014JC010155.

Körtzinger, A. (2003). A significant CO2 sink in the tropical Atlantic Ocean A significant CO2 sink in the tropical Atlantic Ocean associated with the Amazon Plume River plume. *Geophysical Research Letters*, 30, 1–4. http://dx.doi.org/10.1029/2003GL018841.

Kucharski, F., Parvin, A., Rodriguez-Fonseca, B., Farneti, R., Martin-Rey, M., Polo, I., Losada, T. (2016). The teleconnection of the tropical Atlantic to indo-Pacific Sea surface temperatures on inter-annual to centennial time scales: A review of recent findings. *Atmosphere*, 7, 2, 29. https://doi.org/10.3390/atmos7020029.

Kulk, G., Platt, T., Dingle, J., Jackson, T., Jönsson, B. F., Bouman, H. A., et al. (2020). Primary Production, an Index of Climate Change in the Ocean: Satellite-Based Estimates over Two Decades. *Remote Sensing*, 12, 5, 826. https://doi.org/10.3390/rs12050826.

Landschützer, P., Gruber, N., Bakker, D.C.E., Schuster U. (2014). Recent variability of the global ocean carbon sink. *Global Biogeochemical Cycles*, 28, 9, 927–949. https://doi.org/10.1002/2014GB004853.

This article is protected by copyright. All rights reserved.

Accepted Article

Landschützer, P., Laruelle, G. G., Roobaert, A., and Regnier, P. (2020). A uniform pCO_2 climatology combining open and coastal oceans, *Earth System Science Data*, 12, 2537–2553. https://doi.org/10.5194/essd-12-2537-2020.

Lefèvre, N., Diverrès, D., Francis, G. (2010). Origin of CO_2 undersaturation in the western tropical Atlantic. *Tellus B: Chemical and Physical Meteorology*, 62, 595–607. http://dx.doi.org/10.1111/j.1600-0889.2010.00475.x.

Lefèvre, N., Urbano, D.F., Diverrès, D., Francis, G. (2014). Impact of physical processes on the seasonal distribution of the fugacity of CO_2 in the western tropical Atlantic. *Journal of Geophysical Research*, 119, 646–663. https://doi.org/10.1002/2013JC009248.

Lefèvre, N., Flores Montes, M., Gaspar, F.L., Rocha, C., Jiang, S., De Araújo, M.C., Ibánhez, J.S.P. (2017). Net heterotrophy in the Amazon continental shelf changes rapidly to a sink of CO_2 in the outer Amazon plume. *Frontiers in Marine Science*, 4, 278. https://doi.org/10.3389/fmars.2017.00278.

Lefèvre, N., Tyaquiçã, P., Veleda, D., Perruche, C., & Van Gennip, S. J. (2020). Amazon River propagation evidenced by a CO_2 decrease at 8° N, 38° W in September 2013. *Journal of Marine Systems*, *211*, 103419, https://doi.org/10.1016/j.jmarsys.2020.103419.

Liang, Y.C., Lo, M.H., Lan, C.W., Seo, H., Ummenhofer, C. C., Yeager, S., et al. (2020). Amplified seasonal cycle in hydroclimate over the Amazon River basin and its plume region. *Nature Communications*, 11, 1, 4390. https://doi.org/10.1038/s41467-020-18187-0.

Liutti, C. C. et al. (2021). Sea surface CO_2 fugacity in the southwestern South Atlantic Ocean: An evaluation based on satellite-derived images. *Marine Chemistry*, 104020. https://doi.org/10.1016/j.marchem.2021.104020.

Louchard, D., Gruber, N., & Münnich, M. (2021). The impact of the Amazon on the biological pump and the air-sea CO2 balance of the Western Tropical Atlantic. *Global Biogeochemical Cycles*, 35, 6, e2020GB006818. https://doi. org/10.1029/2020GB006818.

Lübbecke, J. F., Durgadoo, J. V., & Biastoch, A. (2015). Contribution of increased Agulhas leakage to tropical Atlantic warming. *Journal of Climate*, 28, 24, 9697-9706. https://doi.org/10.1175/JCLI-D-15-0258.1.

Lueker, T. J., Dickson, A. G., & Keeling, C. D. (2000). Ocean pCO_2 calculated from dissolved inorganic carbon, alkalinity, and equations for K1 and K2: validation based on laboratory measurements of CO_2 in gas and seawater at equilibrium. *Marine chemistry*, 70,1-3, 105-119. https://doi.org/10.1016/S0304-4203(00)00022-0.

Marengo, J. A., & Espinoza, J. C. (2016). Extreme seasonal droughts and floods in Amazonia: causes, trends and impacts. *International Journal of Climatology*, 36, 1033–1050, https://doi.org/10.1002/joc.4420.

Meinshausen, M., Nicholls, Z. R., Lewis, J., Gidden, M. J., Vogel, E., Freund, M., et al. (2020). The shared socio-economic pathway (SSP) greenhouse gas concentrations and their extensions to 2500. *Geoscientific Model Development*, 13, 8, 3571-3605. https://doi.org/10.5194/gmd-13-3571-2020.

This article is protected by copyright. All rights reserved.

Accepted Article

Mehrbach, C., Culberson, C. H., Hawley, J. E., & Pytkowicz R. M. (1973). Measurements of the apparent dissociation constants of carbonic acid in seawater at atmospheric pressure. *Limnology and Oceanography*, 18, 897– 907. https://doi.org/10.4319/lo.1973.18.6.0897.

Millero, F. J. (2010). Carbonate constants for estuarine waters. *Marine and Freshwater Research*, 61, 2, 139-142. https://doi.org/10.1071/MF09254.

Millero, F.J., Graham, T.B., Huang, F., Bustos-Serrano, H., Pierrot, D. (2006). Dissociation constants of carbonic acid in seawater as a function of salinity and temperature. *Marine Chemistry*, 100, 80–94. http://dx.doi.org/10.1016/j.marchem.2005.12.001.

Moura, R. L., Amado-Filho, G. M., Moraes, F. C., Brasileiro, P. S., Salomon, P. S., Mahiques, M. M. et al. (2016). An extensive reef system at the Amazon River mouth. *Science Advances*, 2, 4, e1501252. http://dx.doi.org/10.1126/sciadv.1501252.

Mu, L., Gomes, H. D. R., Burns, S. M., Goes, J. I., Coles, V. J., Rezende, C. E., et al. (2021). Temporal Variability of Air- Sea CO2 flux in the Western Tropical North Atlantic Influenced by the Amazon River Plume. *Global Biogeochemical Cycles*, *35*, 6, e2020GB006798. https://doi.org/10.1029/2020GB006798.

Neumann-Leitão, S., Melo, P. A. M. C., Schwamborn, R., Diaz, X. F. G., Figueiredo, L. G. P., Silva, A. P., et al. (2018). Zooplankton from a reef system under the influence of the Amazon River plume. *Frontiers in microbiology*, 9, 355. https://doi.org/10.3389/fmicb.2018.00355.

Olsen, A., Lange, N., Key, R. M., Tanhua, T., Bittig, H. C., Kozyr, A., et al. (2020). GLODAPv2.2020 – the second update of GLODAPv2. doi:10.5194/essd- 2020- 165.

Orselli, I. B. M., Kerr, R., Azevedo, J. L. L. d., Galdino, F., Araujo, M. & Garcia, C. A. E. (2019). The sea-air CO_2 net fluxes in the South Atlantic Ocean and the role played by Agulhas eddies. *Progress in Oceanography*, 170, 40-52. https://doi.org/10.1016/j.pocean.2018.10.006.

Orselli, I. B. M., Goyet, C., Kerr, R., Azevedo, J. L. L. de Araujo, M., Galdino, F., et al. (2019). The effect of Agulhas eddies on absorption and transport of anthropogenic carbon in the South Atlantic Ocean. *Climate*, 7, 6, 84. https://doi.org/10.3390/cli7060084.

Park, G.-H., & Wanninkhof, R. (2012). A large increase of the CO2 sink in the western tropical North Atlantic from 2002 to 2009. Journal of Geophysical Research, 117, C08029. https://doi.org/10.1029/2011JC007803.

Pierrot, D. E. L., & Wallace, D. W. R. (2006). MS Excel Program Developed for CO2 System Calculations. ORNL/CDIAC-105a. Carbon Dioxide Information Analysis Center, Oak Ridge National Laboratory, U.S. Department of Energy, Oak Ridge, Tennessee, doi: 10.3334/CDIAC/otg.CO2SYS_XLS_CDIAC105a.

Richardson, P.L., & Reverdin, G. (1987). Seasonal Cycle of Velocity in the Atlantic North Equatorial Countercurrent as Measured by Surface Drifters,Current Meters, and Ship Drifts. *Journal of Geophysical Research*, 92, C4, 3691-3708. https://doi.org/10.1029/JC092iC04p03691.

This article is protected by copyright. All rights reserved.

Accepted Article

Rodrigues, R.R., Rothstein, L.M., Wimbush, M. (2007). Seasonal variability of the South Equatorial Current bifurcation in the Atlantic Ocean: A numerical study. *Journal of Physical Oceanography*, 37, 16-37. https://doi.org/10.1175/JPO2983.1.

Salisbury, J., Vandemark, D., Campbell, J., Hunt, C., Wisser, D. et al. (2011). Spatial and temporal coherence between Amazon River discharge, salinity, and light absorption by colored organic carbon in western tropical Atlantic surface waters. *Journal of Geophysical Research: Oceans*, 116, C00H02. https://doi.org/10.1029/2011JC006989.

Sathyendranath, S., Jackson, T., Brockmann, C. et al. (2021). ESA Ocean Colour Climate Change Initiative (Ocean_Colour_cci): Version 5.0 Data. NERC EDS Centre for Environmental Data Analysis, 19 May 2021. http://dx.doi.org/10.5285/1dbe7a109c0244aaad713e078fd3059a.

Sarmiento, J. L., and N. Gruber (2006), Ocean Biogeochemical Dynamics, Princeton Univ. Press, Princeton, Woodstock.

Schlitzer, R. (2018). Ocean Data View, v. 5.3.0. https://odv.awi.de.

Silva, M., Araujo, M., Servain, J., Penven, P., Lentini, C.A.D. (2009). High-Resolution Regional Ocean Dynamics Simulation in the Southwestern Tropical Atlantic. *Ocean Modelling*, 30, 256-269. https://doi.org/10.1016/j.ocemod.2009.07.002.

Smith, W. O., Jr, & Demaster, D. J. (1996). Phytoplankton biomass and productivity in the Amazon River plume: Correlation with seasonal river discharge. *Continental Shelf Research*, 16, 3, 291–319. https://doi.org/10.1016/0278-4343(95)00007-N.

Souza, A. D., Kerr, R., & Azevedo, J. D. (2018). On the influence of subtropical mode water on the South Atlantic Ocean. *Journal of Marine Systems*, 185, 13–24 https://doi.org/10.1016/j.jmarsys.2018.04.006.

Sweeney, C., Gloor, E., Jacobson, A. R., Key, R. M., McKinley, G., Sarmiento, J. L., & Wanninkhof, R. (2007). Constraining global air- sea gas exchange for CO_2 with recent bomb 14C measurements. *Global Biogeochemical Cycles*, 21, 2. https://doi.org/10.1029/2006GB002784.

Takahashi, T., Sutherland, S. C., Sweeney, C., Poisson, A., Metzl, N., Tillbrook, B., Bates, N., Wanninkhof, R., Feely, R. A., Sabine, C., Olafsson, J., Nojiri Y. Global sea–air CO_2 flux based on climatological surface ocean pCO_2, and seasonal biological and temperature effects. *Deep Sea Research Part II: Topical Studies in Oceanography*, 49 (2002), 1601–1622. https://doi.org/10.1016/S0967-0645(02)00003-6.

Takahashi, T., Sutherland, S.C., Wanninkhof, R., Sweeney, C., Feely, R.A., Chipman, D.W., de Baar, H.J.W. (2009). Climatological mean and decadal change in surface ocean pCO_2, and net sea–air CO_2 flux over the global oceans. *Deep Sea Research Part II: Topical Studies in Oceanography*, 56, 554–577. https://doi.org/10.1016/j.dsr2.2008.12.009.

Takahashi, T., Sutherland, S. C., Chipman, D. W., Goddard, J. G., Ho, C., Newberger, T., et al. (2014). Climatological distributions of pH, pCO_2, total CO_2, alkalinity, and CaCO3 saturation in the global surface ocean, and temporal changes at selected locations. *Marine Chemistry*, 164, 95-125. https://doi.org/10.1016/j.marchem.2014.06.004.

This article is protected by copyright. All rights reserved.

Accepted Article

Tyaquiçã, P., Veleda, D., Lefèvre, N., Araujo, M., Noriega, C., Caniaux, G., Servain, J., & Silva, T. (2017). Amazon Plume Salinity Response to Ocean Teleconnections. *Frontier Marine Science*, 4, 250, https://doi.org/10.3389/fmars.2017.00250.

Uppström, L. R. (1974). The boron/chlorinity ratio of deep-sea water from the Pacific Ocean. *Deep Sea Research and Oceanographic Abstracts*, 21, 161–162. https://doi.org/10.1016/0011-7471(74)90074-6.

Utida, G., Cruz, F. W., Etourneau, J., Bouloubassi, I., Schefuß, E., Vuille, M., et al. (2019). Tropical South Atlantic influence on Northeastern Brazil precipitation and ITCZ displacement during the past 2,300 years. *Scientific Reports*, 9, 1, 1698. https://doi.org/10.1038/s41598-018-38003-6.

Valerio, A.M., Kampel, M., Ward, N.D., Sawakuchi, H.O., Cunha, A.C., Richey, J.E. (2021). CO_2 partial pressure and fluxes in the Amazon River plume using in situ and remote sensing data. *Continental Shelf Research*, *215*, 104348. https://doi.org/10.1016/j.csr.2021.104348.

Varona, H. L., Veleda, D., Silva, M., Cintra, M., & Araujo, M. (2019). Amazon River plume influence on Western Tropical Atlantic dynamic variability. *Dynamics of Atmospheres and Oceans*, 85, 1– 15. https://doi.org/10.1016/j.dynatmoce.2018.10.002.

Wanninkhof, R. (1992). Relationship between wind speed and gas exchange. *Journal of Geophysical Research: Oceans*, 97, 7373-7382. https://doi.org/10.1029/92JC00188.

Wanninkhof, R. & McGillis, W. R. (1999). A cubic relationship between air-sea CO_2 exchange and wind speed. *Geophysical Research Letters*, 26, 1889-1892. https://doi.org/10.1029/1999GL900363.

Wanninkhof, R. (2014). Relationship between wind speed and gas exchange over the ocean revisited. *Limnology and Oceanography Methods*, 12, 351–362. https://doi.org/10.4319/lom.2014.12.351.

Wanninkhof, R., Barbero, L. Byrne, R., Cai, W.J., Zhang, H. Z., Baringer, M., & Langdon, C. (2015). Ocean acidification along the Gulf Coast and East Coast of the USA. *Continental Shelf Research*, 98, 54– 71. https://doi.org/10.1016/j.csr.2015.02.008.

Ward, N. D., Keil, R. G., Medeiros, P. M., Brito, D. C., Cunha, A. C., Dittmar, T., et al. (2013). Degradation of terrestrially derived macromolecules in the Amazon River. *Nature Geoscience*, 6, 7, 530–533. https://doi.org/10.1038/ngeo181.

Weiss, R. F. (1974). Carbon dioxide in water and seawater: the solubility of a non-ideal gas. *Marine Chemistry*, 2, 3, 203-215. https://doi.org/10.1016/0304-4203(74)90015-2.

Weiss, R.F., & Price, B.A. (1980). Nitrous oxide solubility in water and seawater. *Marine Chemistry*, 8, 347–359. https://doi.org/10.1016/0304-4203(80)90024-9.

Zeebe, R. and Wolf-Gladrow, D. (2001): CO_2 in Seawater: Equilibrium, Kinetics, Isotopes. *Elsevier Oceanography Book Series*, 65, 346. Amsterdam. ISBN: 0-444-50946-1 and 0-.

This article is protected by copyright. All rights reserved.

Accepted Article